Marine Micropaleontology
January 2023, Volume 178, Pages 102185 (18p.)
https://doi.org/10.1016/j.marmicro.2022.102185
https://archimer.ifremer.fr/doc/00807/91879/

The ciliophoran affinity of *Radiosperma textum*, and its relation to other marine ciliate cysts

Gurdebeke Pieter R. [1, *], Mertens Kenneth [2], Rajter Lubomir [3], Meyvisch Pjotr [1], Potvin Eric [4, 5], Yang Eun Jin [4], André Coralie [1], Pospelova Vera [6], Louwye Stephen [1]

[1] Department of Geology, Ghent University, Krijgslaan 281, S8, 9000 Ghent, Belgium
[2] Ifremer, LITTORAL, F-29900 Concarneau, France
[3] Phycology, Faculty of Biology, University of Duisburg-Essen, Essen, Germany
[4] Korea Polar Research Institute, Division of Polar Ocean Sciences, Incheon, Songdo 406-840, Republic of Korea
[5] Instituto Milenio de Oceanografía, Universidad de Concepción, Concepción, PO Box 160-C, Chile
[6] Department of Earth and Environmental Sciences, University of Minnesota, Minneapolis, MN 55455-0149, USA

* Corresponding author : Pieter R. Gurdebeke, email address : pieter.gurdebeke@ugent.be

Abstract :

The acritarch genus Radiosperma has been reported from plankton and sediments since the late 19th century, with suggested biological affinities ranging from invertebrate eggs to tintinnids. Here, the genus description is improved and its two species, Radiosperma corbiferum and Radiosperma textum, are redescribed. Radiosperma textum is shown to be a ciliate cyst related to Askenasia based on new SSU and LSU rRNA sequences. The spatiotemporal distribution and ecology of both species are discussed. The chemical composition is documented based on micro-Fourier Transform Infrared spectroscopy. Furthermore, new SSU and LSU rRNA sequences for several flask shaped ciliate cysts (Fusopsis, Strombidium) are also included in the analysis and the occurrence of fossilizable cysts in the ciliophoran clade is reviewed.

Highlights

► Former acritarch *Radiosperma* and its two species *R. corbiferum* and *R. textum* are redescribed as ciliates. ► *Radiosperma corbiferum* is confined to Baltic and Arctic waters while *R. textum* occurs elsewhere. ► *Radiosperma textum* is a ciliate cyst based on rRNA. ► Ciliate cyst morphology has taxonomic significance.

Keywords : acritarch, affinity, cysts, ciliate, LSU and SSU rDNA

1. Introduction

Among the organic-walled microfossils (i.e. palynomorphs) found in marine sediments, acritarchs are defined as a group of taxa of unknown biological affinity (e.g. Mendelson 1987; Martin 1993; Montenari and Leppig 2003; Mudie et al. 2021). Over time, several acritarch species were attributed to, among others, dinoflagellate cysts (e.g. Evitt 1961), ciliate cysts (e.g. Gurdebeke et al. 2018a), invertebrate eggs (e.g. Van Waveren and Marcus 1993; Cohen et al. 2009) or prasinophycean phycomata (e.g. Wall 1962). In modern sediments, the biological affinity of an acritarch can be revealed through studies of morphology, chemical

composition, culture experiments and molecular phylogeny. However, in older sediments throughout the geological record, approaches are obviously more limited by the rarefaction of viable species and genetic material through time, and inferences can only be made based on morphology and chemical composition of the acritarchs (e.g. Marshall et al. 2005; Cohen et al. 2009).

The production of resting cysts is a life cycle trait that is common in a very diverse group of organisms including planktonic ciliates and is generally triggered by environmental stressors (e.g. Reid and John, 1983; Verni and Rosati 2011; Belmonte and Rubino 2019). Cyst stages may offer clues on the bloom-forming capacity by benthic seeding and the complex life cycle of some species (e.g. Reid 1987; Ichinomiya et al. 2008). Resting cysts have been invoked in explaining enigmatic ciliate biogeographies (e.g. Esteban and Finlay 2004).

Ciliate resting cysts can be very durable, ensuring survival over long time periods (e.g. thousands of years, Shatilovich et al. 2015). This may translate in a good fossilization potential, so unraveling their fossil record potentially improves the understanding of ciliate evolutionary history and fossil marine ecosystems. Unfortunately, although their fundamental role in ciliate biology has been stressed, ciliate resting cysts remain understudied (Reid and John 1983; Kaur et al. 2019). While cyst stages have been studied more intensely for ciliates living in soils and freshwater, the picture is less clear for marine species (Corliss and Esser 1974; Belmonte and Rubino 2019), except for species referred to as “tintinnids”, i.e. loricate Choreotrichida (Spirotricha, Oligotrichea) (Reid and John 1978, 1983; Kamiyama 2013). These cysts are typically flask-shaped and are often identified in palynological studies, though species designations are often hampered by morphological convergence of the cysts (e.g. Doherty et al. 2010). In all, resting cyst formation is known for less than 100 marine ciliate species, and the detailed life cycle is known for only a few of them. Supplementary Information SI1 summarizes the marine ciliate cysts that are published with illustrations.

Recently, Gurdebeke et al. (2018a) showed the ciliate affinity of *Halodinium* Bujak, 1984 and *Hexasterias* (Cleve) Gurdebeke, 2018, which were previously considered acritarchs, and suggestions were made for the ciliate cyst nature of other acritarchs, such as species belonging to the genus *Radiosperma*.

The genus and species *Radiosperma corbiferum* were introduced in a study of plankton collected in the Barents and Kara Seas by Meunier (1910, p. 95, Pl. 6, 16-18), figuring among his "enigmatic organisms." Earlier, this organism was called *Sternhaarstatoblast* (literally "star-haired statoblast") by Hensen (1887). A second species, *Radiosperma textum*, was described by the same author in plankton collected from Belgian coastal water (Meunier 1919, p. 41, Pl. 23, Fig. 21–22). Since it is a conspicuous and easily recognizable taxon, congeners of *Radiosperma*, and especially *R. corbiferum*, have often been reported from both plankton and sediments. The biological affinity of *R. corbiferum* remained enigmatic until now, with various assumptions being made by different authors. Hensen (1887) suggested that *R. corbiferum* was a bryozoan resting spore and Meunier (1919) described *R. textum* as an animal egg. Reid (1972) suggested *R. textum* to be a rotiferan egg and Telesh et al. (2009) reported *R. corbiferum* as a heliozoan. Interestingly, Ekman and Fries (1970) proposed that *R. corbiferum* is the cyst of the freshwater suctorian ciliate *Staurophrya elegans*, and Mudie et al. (2010) assigned *Radiosperma*-type cysts to the tintinnids. Finally, Gurdebeke et al. (2018a) speculated about a ciliate affinity based on similarities in morphology and macromolecular composition with *Hexasterias* and *Halodinium*, but no molecular data were available to confirm this at this time.

Here, we review the taxonomy and ecology of *Radiosperma*, infer its biological affinity by means of molecular phylogenies using SSU and LSU rRNA sequences and further document the macromolecular composition of the cyst wall through micro-FTIR

spectroscopy. Furthermore, new sequence data for a suite of flask-shaped cysts are presented, along with a review on the occurrence of fossilizable resting cysts in the phylum Ciliophora.

2. Material and methods

2.1 Sampling and imaging

Sampling. Specimens of *Radiosperma* sp., cysts of *Strombidium* sp., *Fusopsis* spp. and an indeterminate ciliate cyst were extracted from surface sediment samples taken with a Petite Ponar grab from the Vilaine Bay and at Pornichet (Loire-Atlantique, France) (Table 1, Fig. 1). Other specimens of *Fusopsis* sp. were extracted from surface sediment samples collected from the Chukchi Sea on board the IBRV Araon during the cruise ARA06C and from the west coast of Greenland in the Labrador Sea on board the RV Maria S. Merian during the cruise MSM45 with a box corer (Table 2, Fig. 1). The sediment was stored in the dark at 4 °C until further analyses. For imaging, additional specimens of *Radiosperma* sp. were retrieved from surface sediments from Gironde (France), Saanich Inlet, near Brentwood Bay (British Columbia, Canada) and the Beaufort Sea (Table 1, Fig. 1).

Isolation. To concentrate *Fusopsis* spp. cysts, between 1 and 2 cm^3 of sediment was sonicated for 1 min in filtered seawater and sieved through a 100 µm mesh size Nytex filter. The residue fraction was observed with an inverted transmitted light microscope Olympus IX73 (Tokyo, Japan). For all other species, approximately 1.0 cm^3 of wet sediment was immersed in filtered seawater prior to ultrasonication in a bath (60 s) and rinsing through a 20 µm meshed nylon net using filtered seawater. The cyst fraction was separated from this residue using heavy liquid sodium polytungstate (density = 1.3 g cm^{-1}) (Bolch 1997).

Light microscopy. The cysts were transferred individually into a drop of filtered seawater framed by a vinyl tape on a glass microscope slide. The cells were sealed by applying silicon grease on the vinyl frame and covering the latter with a coverslip (modified

from Horiguchi et al. 2000). Individual cysts were observed at 200× with an Axio Imager A2 microscope (Carl Zeiss Microscopy GmbH, Göttingen, Germany). The photomicrographs were obtained with an AxioCam HRc digital camera (Carl Zeiss Microscopy GmbH, Göttingen, Germany).

Scanning electron microscopy. For scanning electron microscopy, cysts of *Fusopsis* spp. were washed in Milli-Q® Direct 8 water (EMD Millipore, Darmstadt, Germany). The cysts were then dehydrated in an ascending ethanol series (10%, 30%, 50%, 70%, 90%, 100%). The cells were dried using a critical point dryer (SPI supplies, SPI-DRY regular, West Chester, PA, USA). Finally, the cysts were mounted on stubs, sputter coated with gold-palladium (Cressington 108auto, Cressington Scientific Instruments Ltd., Watford, UK), and observed with a low vacuum scanning electron microscope (JSM-6610LV, JEOL, Tokyo, Japan). For field-emission SEM imaging of *Radiosperma*, cysts were picked with a micropipette from the residue and mounted on polycarbonate membrane filters (Millipore, Billerica, MA, USA, GTTP Isopore, 0.22 lm pore size), air-dried and sputter-coated with gold. The micrographs were obtained using a Zeiss SIGMA300 Gemini field emission SEM at the Station de Biologie Marine (Concarneau, France). Other specimens were photographed with a Jeol 6400 scanning electron microscope at Ghent University.

2.2 DNA amplification and sequencing

For *Fusopsis,* the living cysts were washed in three drops of Milli-Q water and broken with a glass micropipette. Drops containing cellular content were then placed in microtubes and amplified directly.

Amplicons of the SSU rDNA and LSU rDNA were obtained following nested PCR protocols. In the first PCR round final, mix concentrations were as follows: 1X PCR Ex Taq buffer (Takara Bio Inc., Seoul, Korea), 0.2 mM of dNTP (Takara Bio Inc., Seoul, Korea), 0.4

µM of each primer, and 0.025 U μL^{-1} of Ex Taq DNA polymerase (Takara Bio Inc., Seoul, Korea). EUKA and 28S-4R primers (Medlin et al. 1988, Moreira et al. 2007) were used in the first round to amplify the genes coding for the SSU rRNA and LSU rRNA in a final volume of 50 µL. The PCRs were conducted using a thermal cycler (Takara Bio Inc., model TP350, Australia, Victoria) and the following protocol: one activation step of 2 min at 95°C, followed of 35 cycles at 95°C for 20 s, 57°C for 40 s, and 72°C for 4 min, and a final elongation step at 72°C for 10 min. A volume of 1 µL of the first PCR step was used as template for the second PCR round using the same mix. Individual reactions in a final volume of 50 µL were produced with these primer pairs and their corresponding annealing temperature (AT) to produce amplicons of the gene coding for the SSU rRNA and LSU rRNA: EUKA/EU929R (AT=52°C), CS322F/EU929R (AT=51°C), Pro+930/EUKB (AT=44°C), NSR951F (5'-GCGAAAGCATTYRCCAA-3', design from E.-NSR951)/EUKB (AT=43°C), 28S-1F/28S-1611R (AT=48°C), 28S-1F/Rev2 (AT=5[illegible]°C), 28S-568F/28S-3R (AT=57°C), 28S-2F/28S-3R (AT=47°C), and 28S-568F/28S-1611R (AT=53°C) (Medlin et al. 1988; Gong et al. 2007; Moreira et al. 2007; Sonnenberg et al. 2007; Mangot et al. 2013; Shimano et al. 2012; Kim et al. 2013). The second round of PCR was as follows: one activation step at 95°C for 2 min, followed by 35 cycles at 95°C for 20 s, AT for 40 s, and 72°C for 1 min, and a final elongation step at 72°C for 5 min.

Positive and negative controls were used for all amplification reactions. The size of the amplicons was verified on a 1.0% agarose gel. Products were visualized under a UV lamp. The PCR products were purified using the Doctor Protein MG™ PCR SV DNA purification kit (MGmed, Inc., Seoul, Korea) according to the manufacturer's instructions. The purified PCR products were sent to Macrogen Inc. (Seoul, Korea) for sequencing on an ABI PRISM® 3700 DNA Analyzer (Applied Biosystems, Foster City, CA, USA) with the primers used in the second round of PCR.

For *Radiosperma* and the other taxa, a similar method was used which is detailed by Gurdebeke et al. (2018a). The cyst-based 18S SSU rRNA sequences are deposited in GenBank under the accession numbers OP288116 (*Radiosperma textum*), KX576664, KX576665 and KX576666 (*Fusopsis* sp., Labrador Sea), KX576667 and KX576668 (*Fusopsis* sp., Chukchi Sea), OP288114 (*Fusopsis* sp., Vilaine Bay); 28S LSU rRNA sequences as OP288115 (*Radiosperma textum*), KX576669, KX576670, and KX576671 (*Fusopsis* sp., Labrador Sea), KX576672, KX576673 and KX576674 (*Fusopsis* sp., Chukchi Sea), OP288113 (Ciliate cyst sp. indet.); SSU-ITS-LSU rRNA sequences as OP288117 (*Strombidium biarmatum*).

2.3 Sequence alignments and phylogenetic analyses

All multiple sequence alignments were built using GUIDANCE2 (Sela et al. 2015) with the MAFFT algorithm and a progressive FFT-NS-1 aligning strategy. The sequences were then manually trimmed based on the SSU-rRNA or LSU-rRNA gene primers (Medlin et al. 1988; Jerome and Lynn 1996) using BioEdit v7.2.5 (Hall 1999).

Phylogenetic trees were inferred using Maximum Likelihood (ML) and Bayesian Inference (BI) methods and applying the GTRGAMMA model of evolution exclusively. ML analyses were performed by RAxML v8.2.12 using the SPR tree-rearrangement. Bipartition support came from 1000 bootstrap replicates. BI analyses were performed by MrBayes v3.2.7a (Ronquist et al. 2012), using four independent chains running 20 million generations each, and sampling every one thousand. The burn-in was specified as 25% of the first sampled trees. Trees were visualized in FigTree v1.2.3 (Rambaut 2009).

2.4 Geochemical analysis of cyst wall composition

For micro-FTIR geochemical analysis of *Radiosperma* spp., palynological residue was used from Vilaine Bay, Diana lagoon, Akkeshi Bay, Dee Estuary and Chesapeake Bay. Between palynological processing and the preparation for micro-FTIR, these residues were stored in cool and dark conditions without adding conservation chemicals. The palynological residues were treated as described in Gurdebeke et al. (2018a). They were ultrasonicated for 30s and rinsed three times with organic solvents (methanol and dichloromethane, 1:1 in volume) and Milli-Q water over a 20 µm mesh to remove polar and apolar compounds that might have adhered to the outside of the cyst walls. Visually clean individual cysts were manually isolated and placed on an Au-coated mirror. Specimens were analyzed with a Bruker Hyperion 2000 microscope coupled to a Bruker Vertex 80v FTIR spectrometer at the Department of Solid State Sciences of Ghent University. Magnification of the microscope was set at 15× and the aperture at 100×100 µm. The combination of detector (liquid N_2 cooled MCT detector), source (Globar) and beamsplitter (KBr) settings restrict the effective infrared spectral range examined to ~4000–650 cm^{-1}. All presented spectra are recorded in reflection mode (deposits on the Au mirror), at a resolution of 2 cm^{-1}, and averaged over 100 scans. Data were analyzed with OPUS© spectroscopy software (Bruker 2014). The presented absorbance spectra were obtained after background (direct reflection on the Au mirror) subtraction, atmospheric correction and baseline correction using a rubberband correction method using polynomes.

3. Results

3.1 Taxonomy

Phylum Ciliophora Doflein, 1901

Subphylum Inframacronucleata Lynn 1996

Class *incertae sedis*

Genus *Radiosperma* Meunier, 1910 emend.

Synonymy.

1910 *Radiosperma* – Meunier, Microplankton, p. 95, pl. 6, 16–18 (original description of genus).

Type species. *Radiosperma corbiferum* Meunier, 1910.

Improved diagnosis. Organic walled transparent cyst with a circular outline in polar view. The spherical, oblate to conical central body has a double wall and a polar circular excystment pore (pylome, cyclopyle) with a detached operculum. Processes are equatorially or subequatorially attached to the outer wall of the central body. Processes form a collar around the central body that is planar or recurved away from the side of the excystment pore.

Remarks. The processes in the equatorial plane may be recurved in a particular polar direction resembling a parachute, as suggested by several authors (e.g. Leegaard 1920).

Species classified in *Radiosperma*. *Radiosperma corbiferum* Meunier, 1910, *Radiosperma textum* Meunier, 1919.

Comparison. Cysts of the genus *Hexasterias* have a similar discoidal shape and circular excystment pore, but have a smaller number (4 to 9, Gurdebeke et al., 2018a) of wider, hollow processes extending radially in the equatorial plane. Cysts of the genus *Halodinium* are flattened, have a smaller excystment pore, the flange is not built up of discrete processes and lines up with the base of the central body. Phycomata of the phototrophic chlorophytes *Pterosperma* and *Trochiscia* lack a circular pylome and have a continuous flange in the equatorial plane. This also applies to eggs of the copepod *Tortanus*, which are also much bigger (e.g. ~270 µm in Johnson 1934), and for the morphologically similar acritarchs *Pterospermella*.

Radiosperma corbiferum Meunier, 1910 emend.

Pl. 1, Fig. 1–2, 5–6; Pl. 2, Fig. 5.

Synonymy.

1887 'Sternhaarstatoblast' – Hensen, Ber. Komm. Wiss. Unters. Meere 5, 66, pl. IV, fig. 23–24 (first illustration).

1910 *Radiosperma corbiferum* sp. n. – Meunier, Microplankton, p. 96, pl. 6, 16–18 (original description).

1920 *Radiosperma corbiferum* – Leegaard, Acta Soc. Sci. Fennicæ 48, p. 30–31, fig. 30 (record from the Finland Baltic coast, with illustration).

1970 Resting cyst of *Staurophyra elegans* – Ekman and Fries, Geol. Fören. Stockh. Förh. 92, 214–224, p. 221, fig. 6 (misidentification; first report of a fossil occurrence from Sweden, with illustration).

1988 "Organismetype A" – Gundersen, Dissertation, pl. 4, fig. 4 (record from surface sediments in the Baltic Sea, with illustration).

1994 "Sternhaarstatoplast" [*sic*] – Nehring, Ophelia 39, fig. 3M (record from Kiel Bight, Germany, with illustration).

1998 *Radiosperma corbiferum* – Kunz-Pirrung, Ber. Polarforsch. 281, p. 98, pl. 4, fig. 2, 5 (record from the Laptev Sea, with illustration).

2009 "unidentified species of Heliozoa" – Telesh et al., Meereswiss. Ber. 76, pl. 5.3.35, fig. 4,5 (record from the Baltic Sea, with illustration).

2018 *Radiosperma corbiferum* – Gurdebeke et al., Eur. J. Protist., p. 129 (micro-FTIR spectra from the Baltic Sea, with illustration).

2020 *Radiosperma corbiferum* – Pienkowski et al., Mar. Micropaleontol. 156, fig. 4b (record from the Canadian Arctic, with illustration).

Improved diagnosis. Oblate to conical central body with a polar excystment pore. The central body is surrounded by a flat equatorial ring-shaped zone. Straight to slightly curved

processes which are consistently connected by Y-shaped furcations about halfway their length and distally free.

Description. Small ridges on the central body start tangentially to the pylome margin and spiral away towards the equatorial plane, where they grade into the processes. The processes, around 86 in number (N=2), bifurcate about halfway their length in the equatorial plane, and join with the adjacent processes. Process terminations are free, though they may be recurved towards each other (Pl. 1, Fig. 5). Occasionally, vacuoles are formed near the furcations of the processes (Pl. 1, Fig. 5).

Dimensions. Morphometric data in Table 2 is compiled from Hensen (1887), Leegaard (1920), Gundersen (1988), Nehring (1994) and Kunz-Pirrung (1998) and Mudie et al. (2021). Total diameter is 90,0–200,0 µm (average 159,6 µm), the central body is 42,0–55,5 µm (average 44,7 µm) and the pylome is 25,0–40,0 µm (average 38,0 µm). Own measurements: total diameter 184 µm, central body 52.2 µm, flange width 57.6 µm (N=2).

Comparison. *Radiosperma textum* and has a different organization of the equatorial flange and has a smaller total diameter (average 102,6 µm), central body diameter (average 44,7 µm), flange width (average 28,3 µm) and pylome size (average 25,2 µm), though there is some range overlap (Table 2).

Radiosperma textum Meunier, 1919 emend.

Pl. 1, Fig. 3–4, 7–13; Pl. 2, Fig. 1–4, 6, 7.

Synonymy.

1907 'similar to Hensen's Sternenhaar-statoblast' – Wright, Contrib. Can. Biol. Fish. 1, p. 9, pl. 3, fig. 3 [not fig. 4, as noted in text and plate caption] (first illustration).

1919 *Radiosperma textum* – Meunier, Mém. Mus. r. hist. nat. Belg. 8, p. 41, pl. 23, fig. 21–22 (description of the species from the Belgian coast, with illustration).

1928 *Radiospermum textum* – Wailes, Vancouver Museum and Art Notes, p. 30, pl. 8, fig. 39–40 (record from British Columbia, with illustration).

1972 Sternhaarstatoblast – Reid, PhD thesis: p. 23, pl. 23, fig. 1–3 (record from the British Isles, first photomicrograph).

1983 *Radiosperma textum* – Vermeiren, thesis, p. 64, pl. 4, fig. 6 (record from SE of Schiermonikoog, the Netherlands, with illustration)

1999 'Protiste sp. 2' – Bérard-Thériault et al., Guide de l'identification: p. 323, pl. 149, Fig. b (record from the Gulf of Saint-Lawrence, with illustration)

2005 *Radiosperma corbiferum* – Head et al., Quat. Int. 130, p. 20, 22, fig. 12, r–s, fig. 13, a (oldest substantiated fossil record, Eemian of the southern Baltic, with illustration).

2006 *Radiosperma corbiferum* – Sorrel et al., Palaeogeogr. Palaeoclimatol. Palaeoecol. 234, p. 312, fig. 6.9–6.12, fig. 10.8 (record from the Holocene of the Aral Sea, with illustration).

2010 *Radiosperma corbiferum* – Pospelova et al., Marine Micropaleontol. 75, pl. VIII, fig. 8 (sediment trap record from the Strait of Georgia, with illustration).

2011 *Radiosperma corbiferum* – Price and Pospelova, Mar. Micropaleontol. 80, pl. 6, fig. 7 (sediment trap record from Saanich Inlet, with illustration).

2012 *Radiosperma corbiferum* – Candel et al., Mar. Micropaleontol. 96-97, fig. 3.12, (rare record from the southern Hemisphere, with illustration).

2013 *Radiosperma corbiferum* – Candel et al., Palynology 37, p. 68, fig. 2.14 (record from the Beagle Chanel, with illustration).

2018 *Radiosperma corbiferum* – Gurdebeke et al., Eur. J. Protist. 66, p. 129, no figures (micro-FTIR spectra from the Brittany and the Irish Sea).

Improved diagnosis. An oblate central body with polar excystment pore is surrounded by a collar that is attached in the equatorial plane. The collar is an evenly spaced lateral reticulate

network is built as a that is formed by two coplanar sets of long, slender and consistently curved processes which meet ±perpendicularly. The outer outline of the flange is irregular.

Description. The three-dimensional shape of the cyst ranges from a nearly flat disk (Pl. 2, Fig. 1) to a cup (Pl. 1, Fig. 8). The pylome is preformed (Pl. 2, Fig. 3) closed by an operculum which bears a very fine ornament consisting of concentric striations (Pl. 2, Fig. 2). Opposite to the pylome, the central body is occasionally observed to bear a second circular opening (Pl. 2, Fig. 1). This second opening is not preformed (Pl. 1, Fig. 8) and is probably created by coincidental damage favored by the concentric ornament.

Around ±80 (N=2) differentially directed processes radiate out from the central body on which they are (sub)equatorially attached. Half of these swirl clockwise (looking from the pylome side) and are on the apical side of the pylome, and another half are counterclockwise oriented on the antapical side. The central body has a finely costate sculpture, which runs tangentially to the pylome margin and swirls out in an anticlockwise fashion until the central body margin, where the minute ridges bend into a more radial direction and transform into the apical set of processes. Distally, the apical set of processes bifurcate, the terminations joining the adjacent processes. The processes are variably interwebbed by finer threads (Pl. 2), towards the central body sometimes closing the space between processes. The processes are distally furcated, mostly bifurcate, rarely trifurcate (Pl. 2). Cell contents include numerous small transparent to yellow lipid bodies (Pl. 1, Fig. 11).

Dimensions. The morphometrics of *R. textum* are given in Table 2. Total cyst diameter 95,3 (102,6) 108,0 µm (N=5); central body diameter 33,2 (44,7) 54,5 µm (N=11); flange width 21,6 (26,3) 33,7 µm (N=7). Pylome diameter 21,7 (25,2) 28,3 µm (N=10), occasional secondary pylome diameter 8,7 (10,2) 13,1 µm (N=3).

Comparison. *Radiosperma corbiferum* can be distinguished based on the organization of its equatorial flange and is generally larger, tough there is some overlap (Table 2).

Class Spirotrichea Bütschli 1889

Order Oligotrichida Bütschli 1887

Fusopsis spp.

Pl. 3, Figs. 1–7.

Spindle-shaped specimens of *Fusopsis* sp. from the Vilaine Bay and the Chukchi and Labrador seas (Pl. 3) were identified based on Meunier (1910) and Reid and John (1978). Total length 371–441 µm, maximum diameter 47–51 µm (N=2).

Strombidium biarmatum Agatha et al., 2005

Pl. 3, Figs. 8–9

The morphological identification of the cyst of *Strombidium biarmatum* was based on Agatha et al. (2005). The cysts are shaped like a round-bottom flask. Size 34×21 µm (N=2), length:width ratio of ~1.6, while Agatha et al. (2005) report 33.4×19.5 µm and a length:width ration of 1.7 on average. Wall colorless and with few, typical rod-shaped, spines, between which dirt can accumulate. A hyaline plug closes the emergence pore.

Ciliate cyst sp. indet.

Pl. 3, Figs 10–11.

An unidentified spherical to flask-shaped cyst is named here as Ciliate cyst indet sp. based on resemblances with other ciliate cysts (see Supplementary Information SI1). The average diameter is 26 µm (N=2).

3.2 Distribution of Radiosperma

Reported occurrences of *Radiosperma* species are mapped in Fig. 3, with indication of species identity when this could be confirmed (Supplementary Information SI2). Based on personal observations, *R. textum* further occurs in surface sediments from the Dee Estuary (Irish Sea), Diana Lagoon (Corsica), Chesapeake Bay (USA), Akkeshi Bay, Lake Saroma (Japan), Qingdao (this study) and Daya Bay, (China) (Table 1). Furthermore, *R. corbiferum* was observed in the Beaufort Sea (Table 1). In a surface sediment sample from Galterö, Sweden, both *R. corbiferum* and *R. textum* were identified (Pl. 2, Fig. 5, 6).

3.3 Molecular phylogeny and biological affinity

Eight new SSU-rRNA and nine new LSU-rRNA sequences of *Strombidium biarmatum*, *Fusopsis* spp. (Labrador Sea, Chukchi Sea and Vilaine Bay, France), *Radiosperma textum*, and Ciliate cyst sp. indet. were used in the SSU-rRNA and LSU-rRNA phylogenetic trees containing each major ciliate taxon and an outgroup from the class Dinophyceae (Fig. 4, 5). Only class Armophorea Lynn, 2004 is not represented in the LSU alignment as its LSU-rRNA sequences from GenBank could not be unambiguously aligned. In both trees, *S. biarmatum* and *Fusopsis* sp. were placed within the Oligotrichida (class Spirotrichea), and *R. textum* was found in a cluster with species of the classes Prostomatea, Plagiopylea and Oligohymenophorea (Fig. 4). The Ciliate cyst sp. indet., which only has a LSU-rRNA gene sequence, represented an early branch in the class Spirotrichea (Fig. 5).

For the closer phylogenetic evaluation of the new sequences, we built the SSU-rRNA Oligotrichia and Prorodontida trees (Fig. 6, 7) and the LSU-rRNA Spirotrichea tree (Fig. 8). In the SSU-rRNA Oligotrichia tree, the *Strombidium biarmatum* was grouped in the family Strombidiidae Fauré-Fremiet 1970, forming a statistically supported clade (96 % ML, 1.00 BI) with *S. biarmatum*, *S. paracapitatum* Song et al. 2015, and *S. basimorphum* Martin and Montagnes, 1993. Also, *Fusopsis* sp. from the Vilaine Bay clustered within the Strombidiidae

creating a moderately supported clade (72 % ML, 0.90 BI) with *Cyrtostrombidium paralongisomum* Tsai et al. 2014 and *C. longisomum* Lynn and Gilron, 1993. Their sister group was represented by other *Fusopsis* sp. populations from the Labrador and Chukchi seas although this relationship was statistically unsupported (<50 % ML, <0.5 BI) (Fig. 6). In the SSU-rRNA Prorodontida tree, *Radiosperma textum* formed a statistically supported clade (99 % ML, 1.00 BI) with *Askenasia* sp. and *Hexasterias problematica* species (Fig. 7). In the LSU-rRNA Spirotrichea tree, the Ciliate cyst sp. indet. was a sister to *Tintinnopsis orientalis* and *Eutintinnus lususundae* in the subclass Choreotrichia (Fig. 8).

3.4 Geochemical composition through micro-FTIR

A total of 25 new micro-FTIR spectra of *Radiosperma textum* cysts have been recorded from five locations over the Northern Hemisphere: two from Vilaine Bay, one from Diana lagoon, 11 from Akkeshi Bay, four from Dee Estuary and six from Chesapeake Bay. Normalized and averaged spectra are represented in Fig. 9. The individual spectral data are available in supplementary information SI 3.

4 Discussion

4.1 Phylogenetic position and redescription of Radiosperma

From a literature review, it seems that considerable confusion exists between the species *Radiosperma corbiferum* and *R. textum*, with many authors misidentifying the latter species as the former. These species have now been morphologically untangled as *R. corbiferum* (sensu stricto) and *R. textum*, mainly distinguished by the organization of the processes, and also by their size, which, however, shows some overlap. No morphological gradation was observed between *R. corbiferum* and *R. textum*, suggesting they are not merely ecophenotypic

endmembers of one species. As molecular sequences are only available for *R. textum*, the genetic separation cannot be confirmed for now.

The new rDNA (SSU or LSU) sequence extracted from *Radiosperma textum* reveals a position among the ciliophoran classes Prostomatea, Plagiopylea and Oligohymenophorea (Figs. 4, 5). The sequences of *R. textum* formed a fully supported clade with *Hexasterias problematica* and *Askenasia* sp. in the vicinity of the family Balanionidae Small and Lynn, 1985 (Fig. 7). Further elucidating of the phylogenetic position of *R. textum* requires improved taxonomic sampling and is beyond the scope of this paper. The closest relation is found with *Askenasia* sp., with a difference of only 2 basepairs in SSU rRNA. Gurdebeke et al. (2018a) already suggested that *R. textum* is closely related to *H. problematica* based on their similar cyst morphology and cyst wall composition.

The incertae sedis genus *Askenasia* was described by Blochmann (1895) and presently includes five species, with *Askenasia volvox* (Eichwald 1952) Kahl 1930 as type species. While the used sequence of *Askenasia* sp. was obtained by Liu et al. (2015) from coastal waters, congeners are also known from freshwater habitats. Resting cysts of this family are documented only for the freshwater species *A. volvox*, which has two shell-like parts ornamented with spines (Penard 1922, Krainer and Foissner 1990). The clade of *Radiosperma* and *Askenasia* is sister to *Hexasterias* and *Halodinium*, suggesting that cyst formation may be a shared characteristic in this group.

Askenasia species have been observed in plankton in conditions similar to those in which *Radiosperma* occurs, e.g. in the Baltic Sea (Mironova et al. 2014) and around the Atlantic and Pacific oceans (Earland and Montagnes 2002). At this point the relation between *Radiosperma* and *Askenasia* is not clear, e.g. whether the ciliates that have *Radiosperma* as a cyst are species of *Askenasia*. In the latter case, the species should be synonymized. Since *Askenasia* was described earlier by Blochmann (1895), it would receive priority over

Radiosperma. Culture experiments of the type species, *A. volvox*, studied from the type locality (freshwater from Haapsalu, Estonia, see Eichwald 1852) could shed some light on this matter.

Molecular sequences of *Radiosperma corbiferum* and more *Askenasia* species are needed to further evaluate the phylogenetic position relative to *R. textum* and *Askenasia*, and the taxonomic resolution needs to be further refined to understand the evolutionary implications for cyst formation. Also, there are probably more *Radiosperma* species to be described. Several forms that resemble *Radiosperma* are undescribed and are illustrated, for example, by Brenner et al. (2005) from the early Holocene of the Baltic Sea, by McCarthy et al. (2021) from NE American Lakes and by Matsuoka & Fishi (2018) from Osaka Bay, Japan. These specimens need further investigation to confirm affinity with *Radiosperma*.

4.2 Distribution and ecology of **Radiosperma**

Based on confirmed occurrences, *Radiosperma corbiferum* sensu stricto appears to be restricted to the Baltic Sea and Arctic coastal waters north of Canada, Greenland and Russia (e.g. Laptev Sea, Kara Sea, Barents Sea) (Fig. 3). On the other hand, *R. textum* appears to be present in coastal and estuarine settings from the temperate Atlantic and Pacific Oceans. The only recorded distribution overlap is at Galterö, at the interface of the Baltic and the North Sea waters (Pl. 2, Fig. 5, 6). For both species, the observations are mainly from coastal and estuarine settings. Observations from the Southern Hemisphere are sparse and limited to the record of *R. textum* in the Beagle Channel (Tierra del Fuego, Argentina) by Candel et al. (2012, 2013, 2017). Alleged observations off Brazil and Peru reported by Brenner (2001) could not be verified, since no illustrations were provided. In all, the sparse records outside Europe and North America are probably biased because the species are not well known/studied.

Heikkila et al. (2016) report the presence of *Radiosperma corbiferum* in two sediment traps deployed in seasonally ice-covered Hudson Bay. Their data show that *R. corbiferum* appear to be abundant during the ice-free seasons, and reaches the highest abundances in July and late fall before the new ice-cover forms. In sediment trap studies from the Strait of Georgia and Saanich Inlet, Pospelova et al. (2010) and Price and Pospelova (2011) found the highest abundances of *R. textum* (reported as *R. corbiferum* with illustrations) in spring and summer, when SSSs are lowest due to increased Fraser River discharge and nutrients are plentiful. Gurdebeke et al. (2018c) found similar patterns in surface sediments from Vancouver Island fjords, where abundances of *R. textum* are highest (up to ~1900 cysts g^{-1}) in the inlets with the highest freshwater input. As such, *Radiosperma* has potential use as a paleoecological indicator of brackish water conditions. Indeed, for example, Ning et al. (2017) report the coincidence of increased abundance of *R. corbiferum* and short-processed cysts of *Protoceratium reticulatum* (Claparede and Lachmann) Bütschli, 1885 in the mid-Holocene of the Baltic Sea. Similarly, Ekman and Fries (1970) used the presence of *R. corbiferum* as an argument for brackish conditions in early Holocene Lake Erken (Sweden), i.e. connection of the lake with the Baltic Sea.

In sediment cores, the abundance of *Radiosperma* often generally decreases deeper down the core (e.g. Pospelova et al. 2006; Bringué et al. 2016; Gurdebeke 2019), which could be related to preservation issues. Reid (1972) found that prolonged acid treatment during palynological preparations is detrimental for the cysts. This suggests that the preservation potential is lower than that of, for example, certain dinoflagellate cysts, and is probably related to the cyst wall chemistry, which differs from that of dinoflagellate cyst walls (Gurdebeke et al. 2018a). Nonetheless, the fossil record of *Radiosperma* may trace back into the Neogene, with Do Couto et al. (2014) reporting a single occurrence from the Messinian (upper Miocene) of the Alboran Sea, but this identification could not be verified since no

illustrations were provided. The oldest substantiated occurrence is that by Head et al. (2005) who report *R. textum* from the Eemian of the southern Baltic Sea (Fig. 3). This contrasts with the exclusive reports of *R. corbiferum* in Holocene sediments and modern plankton of the Baltic Sea (Fig. 3). This may be explained by the fact that the Eemian Baltic Sea was more saline than during the Holocene and the system was intensely disturbed during the last glacial (Head et al. 2005; Miettinen et al. 2014). The dinoflagellate cyst assemblages observed by Head et al. (2005) suggest an influence mainly from the North Sea, which further supports an incursion of the *R. textum* distribution into the Baltic Sea during the Eemian. Further into the Baltic, Eemian records for *Radiosperma* are lacking so the extent of this incursion cannot be estimated. On the other hand, the Eemian seaway connection between the Eastern Baltic and the White Sea (e.g. Miettinen et al. 2014) may explain the observed contemporary distribution of *R. corbiferum*, though Funder et al. (2002) found the connection to be short-lived with a limited exchange of water mass.

The organisms that have *Radiosperma* as a cyst stage can be presumed to be heterotrophic, as is the case for the large majority of the Ciliophora (e.g. Lynn 2008). Indeed, no chloroplasts were observed in any of the living specimens. This is supported by Pienkowski et al. (2020) who found a correlation between abundance of *R. corbiferum* and biogenic silica in surface sediments. It is unknown what organisms form the prey of the ciliate that produces *Radiosperma*, but the distribution of a prey species may hold an explanation for the observed distribution of *R. textum* and *R. corbiferum*. *Radiosperma* itself has been identified as part of food webs. For example, Viherluoto et al. (2000) reported *Radiosperma*, presumably *R. corbiferum*, in mysid shrimp stomach content in the Baltic Sea. Wright (1907) reports similar findings for *R. textum* from Nova Scotia.

4.3 Geochemical composition of Radiosperma

Leegaard (1920) had already experimented on the composition of *Radiosperma corbiferum* from the Baltic Sea and found it to be 'probably chitin'. The first micro-FTIR spectra for *R. textum* were published by Gurdebeke et al. (2018a) (as '*Radiosperma corbiferum*'), who already suggested a ciliate affinity based inter alia on compositional similarities with *Hexasterias problematica* and *Halodinium verrucatum*. With the insights of the present paper, spectra from the Baltic Sea (M5S1, M5S4, M5S9 and M5S18 in Gurdebeke et al. 2018a) were measured on *R. corbiferum*, while the six other spectra reported by these authors were from *R. textum*.

The 25 new micro-FTIR spectra of *Radiosperma textum* presented here (Fig. 9) are concordant with the ones that were published by Gurdebeke et al. (2018a), indicating a conserved composition of the species in estuaries throughout the Northern Hemisphere. From the present data set, no obvious compositional differentiation could be identified between *R. corbiferum* and *R. textum*, but the data set for the former species should be expanded in order to explore this in more detail. The compositional differences with *Hexasterias* and *Halodinium*, as noted by Gurdebeke et al. (2018a), however, remain valid. Taking into account recent insights gained by Meyvisch et al. (2021) on the study of dinoflagellate cysts composition, a more advanced interpretation of a more extensive data set on ciliate cyst wall composition will be the subject of subsequent papers.

4.4 Phylogenetic position of newly sequenced oligotrich and choreotrich cysts

New rRNA (SSU or LSU) sequences of *Strombidium biarmatum*, *Fusopsis* spp. (France, the Labrador and Chukchi Seas) and Ciliate cyst sp. indet. have been assigned to the spirotrich ciliates (Figs. 4, 5). *S. biarmatum* and the specimens of *Fusopsis* from the three locations were placed within the subclass Oligotrichia (class Spirotrichea) (Fig. 6).

In particular, *Strombidium biarmatum* was nested in the family Strombidiidae forming a clade with the existing sequence of *S. biarmatum* (Agatha et al. 2005) and with *S. paracapitatum* and *S. basimorphum*, which have typical *Strombidium* resting cysts (Agatha 2004). This suggests that *S. biarmatum* can be reliably identified based on morphology.

The *Fusopsis* spp. sequences from three localities were placed in the family Cyrtostrombidiidae Agatha, 2004 creating a clade with *Cyrtostrombidium paralongisomum* and *C. longisomum*, for which no resting cysts have been reported. However, the related species *C. boreale*, has cysts with a fusiform shape and a long tail (Kim et al. 2002) that correspond with the *Fusopsis* spp. cysts. The genus *Fusopsis* was established by Meunier (1910), and Kim et al. (2002) related *Fusopsis* collected from sediments with *C. boreale*, which hatched from the cysts in culture experiments. Based on molecular sequences, cysts identified as *Fusopsis* are here shown to also relate to *Cyrtostrombidium*, strengthening the idea of the identification of *Fusopsis* as the cyst stage of *Cyrtostrombidium* ciliates. It is not clear, however, how the diversity of *Fusopsis*-like cysts relates to the diversity of *Cyrtostrombidium*-like ciliates and whether both groups could be synonymized. The complete taxonomic description of the sequenced *Fusopsis* cysts will be published elsewhere.

The Ciliate cyst sp. indet. sequence was nested within the order Choreotrichida in the LSU-rRNA Spirotrichea tree (Fig. 8). This sequence represented a sister to two tintinnids (*Tintinnopsis orientalis* and *Eutintinnus lusundae*) species. However, we could not make a closer phylogenetic assignment as there are not enough LSU-rRNA sequences from the order Choreotrichida. In this situation, Ciliate cyst sp. indet. may belong to the suborder Tintinnina with an external lorica attached to the cell or the aloricate suborder Strobilidiina (Adl et al. 2019).

4.5 Occurrence of fossilizable cysts in the ciliates

The occurrence of resting cysts in the life cycles of ciliates is taxonomically wide-spread but understudied (Foissner et al. 2007; Kaur et al. 2019). Compared with marine genera, freshwater and terrestrial ciliate genera have been relatively well-studied (e.g. Berger 1999, Foissner and Xu 2007; Vdacny and Foissner 2012). Morphologically, these are mostly spherical cysts with varying sculpture and ornamentation (Kaur et al. 2019).

A list of known marine ciliates resting cysts is given in Supplementary Information SI1 and Fig. 10, which are limited to records which are substantiated with illustrations. The majority of the known marine cyst-producing species belong to several families in two orders, Choreotrichida and Oligotrichida (class Spirotrichea), which are also dominant in the ocean plankton (Canals et al. 2020). These groups, often collectively (and wrongly) referred to as 'tintinnids' clearly have the largest known and best described cyst diversity. Besides Choreotrichida and Oligotrichida, cysts are known from the euplotid, stichotrichid, philasterid, prorodontid and heterotrichid groups, and these cysts are typically spheroid or discoid (Supplementary Information SI1).

The fossil record of the tintinnids dates back at least into the Jurassic and probably much older (Dunthorn et al. 2015), but this record is based on the loricae rather than the typically flask-shaped cysts, the latter rarely being reported from deposits older than the Holocene. Nevertheless, ciliate cysts have found (paleo)ecological applications (e.g. Moscatello and Belmonte 2004; Rubino et al. 2013). Furthermore, non-tintinnid ciliate cysts such as *Halodinium* are reported from early Pliocene (Verhoeven et al. 2014) and potentially even early Paleozoic sediments (Benachour et al. 2019), suggesting that at least some ciliate cysts have a certain deep time preservation potential. Future studies on ciliate cyst composition may improve our understanding of their preservation potential and perhaps improve the methods to extract them from sediments.

It is expected that increasing knowledge on marine ciliate life cycles will reveal more cyst species and a dedicated attention for the description of the cyst stage will improve their applicability in (paleo)ecological studies. Also, *incertae sedis* cyst taxa are expected to be linked to ciliates. For example, Rubino and Belmonte (2019) report an acritarch that is apparently intermediate between flask-shaped tintinnids and discoid *Halodinium*-like cysts and for which genetic, life-cycle and compositional information will reveal its taxonomic position, perhaps with the Ciliophora.

Though early authors such as Meunier (1910) defined names for cysts (e.g. *Sphaeropsis*, *Fusopsis*) which were later linked to their active stages (e.g. *Strombidium*, *Cyrtostrombidium*), a dual nomenclature as in dinoflagellate cysts (Ellegaard et al. 2018) is not sanctioned. The cyst-based nomenclature would have historical priority in certain cases (e.g. *Fusopsis* over *Cyrtostrombidium*).

5 Conclusions

Based on rRNA sequences, the former acritarch genus *Radiosperma* is shown here to be a ciliate cyst closely related to *Askenasia*, *Hexasterias* and *Halodinium*. The genus description is emended, and both species are redescribed, the difference being mainly the organization of the processes. *Radiosperma corbiferum* is confined to the Baltic Sea and Arctic coastal waters while *R. textum* occurs in temperate coastal waters in other parts of the world. Both species are indicative of freshwater influence. New micro-FTIR data from *R. textum* cysts suggest constancy of the cyst wall composition in estuaries throughout the Northern Hemisphere.

New sequences for ciliate cysts identified as *Strombidium biarmatum*, *Fusopsis* spp. and Ciliate cyst sp. indet. yield a placement in the ciliophoran phylogenetic tree that agrees with the placement would be expected based on cyst morphology, suggesting that the morphological identification of these ciliate cysts is reliable. Species (and higher taxa) seem

to have a specific cyst shape, suggesting taxonomic importance. A review of marine ciliate resting cysts shows that the phenomenon is taxonomically widespread but mostly known (mainly as flask-shaped cysts) from oligotrich and choreotrich species. Elucidating cyst stages in ciliate life cycles will improve understanding in ciliate biology and ecology and their applicability in (paleo)environmental studies.

Acknowledgments

We would like to thank Nicolas Van Nieuwenhove who provided the sediment from the Labrador Sea used in this study for the genetic analyses. This research was a part of the project titled 'K-AWARE(KOPRI, 1525011760)', funded by the Ministry of Oceans and Fisheries, Korea. Astra Labuce (Latvian Institute of Aquatic Ecology) is thanked for sharing information in *Radiosperma* from the Gulf of Riga. The Regional Council of Brittany, the General Council of Finistère and the urban community of Concarneau-Cornouaille-Agglomération are acknowledged for the funding of the Sigma 300 FE-SEM of the station of Marine Biology in Concarneau. KNM was supported by the project EPICE, financed by Agence de l'Eau Loire-Bretagne and the PhenoMap project, financed by the French National Research Agency (ANR). We are grateful for the constructive manuscript reviews by the editor and two anonymous reviewers.

References

Adl, S.M., Bass, D., Lane, C.E., Luke, J., Schoch, C.L., Smirnov, A., Agatha, S., Berney, C., *et al.*, 2019. Revisions to the Classification, Nomenclature, and Diversity of Eukaryotes. J. Eukaryot. Microbiol. 66, 4–119.

Agatha, S., 2004. Evolution of ciliary patterns in the Oligotrichida (Ciliophora, Spirotricha) and its taxonomic implications. Zoology 107, 153–168.

Agatha, S., Strüder-Kypke, M.C., Beran, A., Lynn, D.H., 2005. *Pelagostrobilidium neptuni* (Montagnes and Taylor, 1994) and *Strombidium biarmatum* nov. spec. (Ciliophora, Oligotrichea): phylogenetic position inferred from morphology, ontogenesis, and gene sequence data. Eur. J. Protistol. 41, 65–83.

Belmonte, G., Rubino, F., 2019. Resting cysts from coastal marine plankton. Oceanography and Marine Biology: An Annual Review 57, 1–88.

Benachour, H.B., Benaslah, M., Gurdebeke, P.R., Kroeck, D.M., Mertens, K.N., Navidi-Izad, N., Raevskaya, E.G., Servais, T., 2019. A review of the acritarch genus *Saharidia* Combaz 1967. AASP-The Palynological Society, 52nd Annual Meeting Abstract Book.

Bérard-Therriault L, Poulin M, Bossé L, 1999. Guide d'identification du phytoplankton marin de l'estuaire et du golfe du Saint-Laurent incluant également certains protozoaires. Can. Spec. Publ. Fish. Aquat. Sci. 128, 1–387

Berger, H., 1999. Monograph of the Oxytrichidae (Ciliophora, Hypotrichia). *Monographiae Biologicae* 78, 1080 p.

Blochmann, F. 1895. Die mikroskopische Thierwelt des Süsswassers, Abtheilung 1: Protozoa. Lucas Grafe & Sillem, Hamburg.

Bolch, C.J.S., 1997. The use of polytungstate for the separation and concentration of living dinoflagellate cysts from marine sediments. Phycologia 37, 472–478.

Brenner, W.W., 2001. Organic-walled microfossils from the central Baltic Sea, indicators of environmental change and base for ecostratigraphic correlation. Baltica 14, 40–51.

Brenner, W.W., 2005. Holocene environmental history of the Gotland Basin (Baltic Sea)—a micropalaeontological model. Palaeogeogr. Palaeoclimatol. Palaeoecol. 220 227–241.

Bringué, M., Pospelova, V., Calvert, S.E., Enkin, R.J., Lacourse, T., Ivanochko, T. 2016. High resolution dinoflagellate cyst record of environmental change in Effingham Inlet

(BC, Canada) over the last millennium. Palaeogeogr. Palaeoclimatol. Palaeoecol. 441, 787–810.

Bruker, 2014. OPUS Spectroscopy Software User Manual. Bruker Optik GmbH, Ettlingen.

Canals, O., Obiol, A., Muhovic, I., Vaqué, D., Massana, R., 2020. Ciliate diversity and distribution across horizontal and vertical scales in the open ocean. Mol. Ecol. 29, 2824–2839.

Candel, M.S., Radi, T., de Vernal, A., Bujalesky, G., 2012. Distribution of dinoflagellate cysts and other aquatic palynomorphs in surface sediments from the Beagle Channel, Southern Argentina. Mar. Micropaleontol. 96–97, 1–12.

Candel, M.S., Borromei, A.M., Martinez, M.A., Bujalesky, G., 2013. Palynofacies analysis of surface sediments from the Beagle Channel and its application as modern analogues for Holocene records of Tierra del Fuego, Argentina. Palynology 37, 62–76.

Candel, M.S., Louwye, S., Borromei, A.M., 2017. Reconstruction of the late Holocene paleoenvironment of the western Beagle Channel (Argentina) based on a palynological analysis. Quat. Int. 442, 2–12.

Cohen, P.A., Knoll, A.H., Kodner, R.B., 2009. Large spinose microfossils in Ediacaran rocks as resting stages of early animals. Proc. Nat. Acad. Sci. 106, 6519–6524.

Corliss, J.O., Esser, S.C., 1974. Comments on the Role of the Cyst in the Life Cycle and Survival of Free-Living Protozoa. Trans. Am. Microsc. Soc. 93, 578–593.

Do Couto, D., Popescu, S.M., Suc, J.P., Melinte-Dobrinescu, M.C., Barhoun, N., Gorini, C., Jolivet, L., Poort, J., Jouannic, G., Auxietre, J.L., 2014. Lago Mare and the Messinian Salinity Crisis: Evidence from the Alboran Sea (S. Spain). 2014. Mar. Pet. Geol. 52, 57–76.

Doherty, M., Tamura, M., Vriezen, J.A.C., McManus, G.B., Katz, L.A., 2010. Diversity of Oligotrichia and Choreotrichia ciliates in coastal marine sediments and in overlying plankton. Appl. Environ. Microbiol. 76, 3924–3935.

Dunthorn, M., Lipps, J.H., Dolan, J.R., Saab, M.A., Aescht, E., Bachy. C., Barría de Cao, M.S., Berger, H. et al., 2015. Ciliates — Protists with complex morphologies and ambiguous early fossil record. Mar. Micropaleontol. 119, 1–6.

Earland, K.A., Montagnes, D.J.S., 2002. Description of a new marine species of *Askenasia* Blochmann, 1895 (Ciliophora, Haptoria), with notes on its ecology. J. Eukaryot. Microbiol. 49, 423-427.

Eichwald, V., 1852. Dritter Nachtrag zur Infusorienkunde Russlands. Bull. Soc. Imp. Naturalistes Moscou 25, 388–536

Ekman, P., Fries, M., 1970. Studies of sediments from Lake Erken, Eastern Central Sweden. Geol. Fören. Stockh. Förh. 92, 214–224.

Ellegaard, M., Head, M.J., Versteegh, G.J.M., 2018. Linking biological and geological data on dinoflagellates using the genus *Spiniferites* as an example: The implications of species concepts, taxonomy and dual nomenclature. Palynology 42 (S1), 221–230.

Esteban, G., F., Finlay, B. J., 2004. Marine ciliates (protozoa) in central Spain. Ophelia 58, 12 –22.

Evitt, W.R., 1961. Observations on fossil dinoflagellates. Micropaleontology 7, 385–420.

Foissner, W., Müller, H., Agatha, S., 2007. A comparative fine structural and phylogenetic analysis of resting cysts in oligotrich and hypotrich Spirotrichea (Ciliophora). Eur.. J. Protistol. 43, 295–314.

Foissner, W., Xu, K., 2007. Monograph of the Spathidiida (Ciliophora, Haptoria). Vol I: Protospathidiidae, Arcuospathidiidae, Apertospathulidae. *Monographiae Biologicae* 81, 485 p.Funder, S., Demidov, I., Yelovicheva, Y., 2002. Hydrography and mollusc faunas

of the Baltic and the White Sea–North Sea seaway in the Eemian. Palaeogeogr. Palaeoclimatol. Palaeoecol. 184, 275–304.

Gao, F., Warren, A., Zhang, Q., Gong, J., Miao, M., Sun, P., Xy, D., Huang, J., Yi, Z., Song W., 2016. The all-data-based evolutionary hypothesis of ciliated protists with a revised classification of the Phylum Ciliophora (Eukaryota, Alveolata). Sci. Rep. 6, 24874.

Gong, J., Kim, S.J., Kim, S.Y., Min, G.S., Roberts, D., Warren, A., Choi, J.K., 2007. Taxonomic redescriptions of two ciliates, *Protogastrostyla pulchra* n. g., n. comb. and *Hemigastrostyla enigmatica* (Ciliophora: Spirotrichea, Stichotrichia), with phylogenetic analyses based on 18S and 28S rRNA gene sequences. J. Eukaryot. Microbiol. 54, 468–478.

Gu, H., Huo, K., Krock, B., Bilien, G., Pospelova, V., Li, Z., Carbonell-Moore, C., Morquecho, L., Ninčević, Ž., Mertens, K.N., 2021 Cyst-theca relationships of *Spiniferites bentorii*, *S. hyperacanthus*, *S. ramosus*, *S. scabratus* and molecular phylogenetics of *Spiniferites* and *Tectatodinium* (Gonyaulacales, Dinophyceae). Phycologia 60, 332–353.

Gundersen, N., 1988. En palynologisk undersøkelse av dinoflagellatcyster langs en synkende salinitetsgradient i recente sedimenter fra Østersjø-området. Cand. Scient. Dissertation, Geologisk Institutt, Universitetet i Oslo.

Gurdebeke, P.R., Mertens, K.N., Takano, Y., Yamaguchi, A., Bogus, K., Dunthorn, M., Matsuoka, K., Vrielinck, H., Louwye, S., 2018a. The affiliation of *Hexasterias problematica* and *Halodinium verrucatum* sp. nov. to ciliate cysts based on molecular phylogeny and cyst wall composition. Eur. J. Protistol. 66, 115–135.

Gurdebeke, P.R., Mertens, K.N., Bogus, K., Marret, F., Chomérat, N., Vrielinck, H., Louwye, S., 2018b. Taxonomic re-investigation and geochemical characterization of Reid's

(1974) species of *Spiniferites* from holotype and topotype material. Palynology 42, S1, 93–110.

Gurdebeke, P.R., Pospelova, V., Mertens, K.N., Dallimore, A., Chana, J. Louwye, S. 2018c. Diversity and distribution of dinoflagellate cysts in surface sediments from fjords of western Vancouver Island (British Columbia, Canada). Mar. Micropaleontol. 143, 12–29.

Gurdebeke, P.R., 2019. Holocene dinoflagellate cysts and other palynomorphs from Northern Hemisphere estuaries. Taxonomy, distribution, geochemistry and palaeoecological application. PhD thesis, Ghent University.

Hall, T.A., 1999. BioEdit: a user-friendly biological sequence alignment editor and analysis program for Windows 95/98/NT. Nucleic Acids Symp. Ser. (,Oxf). 41 95–98.

Head, M.J., Seidenkrantz, M.S., Janczyk-Kopikowa, Z., Marks, L., Gibbard, P.L., 2005. Last Interglacial (Eemian) hydrographic conditions in the southeastern Baltic Sea, NE Europe, based on dinoflagellate cysts. Quat. Int. 130, 3–30.

Heikkilä, M., Pospelova, V., Forest, A., Stern, G.A., Fortier, L., Macdonald, R.W., 2016. Dinoflagellate cyst production over an annual cycle in seasonally ice-covered Hudson Bay. Mar. Micropaleontol. 125, 1–24.

Hensen, V., 1887. Ueber die Bestimmung des Plankton's oder des im Meeretreibende Materials an Pflanzen und Tieren. Fünfter Bericht der Kommission zur wissenschaftlichen Untersuchung der deutschen Meere in Kiel für die Jahre 1882 bis 1886, 12–16, pp. 1–107.

Horiguchi, T., Yoshizawa-Ebata, J., Nakayama, T., 2000. *Halostylodinium arenarium*, gen et sp. nov. (Dinophyceae), a coccoid sand-dwelling dinoflagellate from subtropical Japan. J. Phycol. 36, 960–971.

Ichinomiya, M., Nakamachi, M., Fukichi, M., Taniguchi, A., 2008. Resting cells of microorganisms in the 20–100 µm fraction of marine sediments in an Antarctic coastal area. Polar Sci. 2, 27–32.

Jansegers, P., 2019. Analysis of the macro-molecular composition of palynomorphs in northern hemisphere estuarine surface sediments, with emphasis on intra- and inter-species variability. Unedited master's dissertation, Ghent University, 68 p.

Jerome, C.A., Lynn, D.H., 1996. Indentifying and distinguishing sibling species in the *Tetrahymena pyriformis* complex (Ciliophora, Oligohymenophorea) using PCR/RFLP analysis of nuclear ribosomal data. J. Eukaryot. Microbiol. 43, 492–497.

Johnson, M.W., 1934. The life history of the copepod *Tortanus discaudatus* (Thompson and Scott). Biol. Bull. 67, 182–200.

Kamiyama, T., 2013. Comparative biology of tintinnid cysts. In: Dolan, J.R. et al., *The Biology and Ecology of Tintinnid Ciliates*. Wiley-Blackwell, 171–185.

Kaur, H., Iqbal, S., Inga, E., Yawe, D., 2019. Encystment and excystment in ciliated protists: Multidimensional approach. Curr. Sci. 117, 198–203.

Kim, S.Y., Choi, J.K., Dolan, J.R., Shin, H.C., Lee, S.H., Yang, E.J., 2013. Morphological and ribosomal DNA-based characterization of six Antarctic ciliate morphospecies from the Amundsen Sea with phylogenetic analyses. J. Eukaryot. Microbiol. 60, 497–513.

Kim, Y.O., Suzuki, T., Taniguchi, A., 2002. A new species in the genus Cyrtostrombidium (Ciliophora, Oligotrichia, Oligotrichida): its morphology, seasonal cycle and resting stage. Eur. J. Protistol. 49, 338–343.

Krainer, K.H., Foissner, W., 1990. Revision of the genus *Askenasia* Blochmann, 1895, with proposal of two new species, and description of *Rhabdoaskenasia minima* n. g., n. sp. (Ciliophora, Cyclotrichida). J. Protozool. 37: 414–427.

Kunz-Pirrung, M., 1998. Aquatic palynomorphs: Reconstruction of Holocene sea-surface water masses in the eastern Laptev Sea. Berichte zur Polarforschung 281, 1–117.

Leegaard, C., 1920. Microplankton from the Finnish waters during the month of may 1912. Acta Soc. Scient. Fenn. 48, 1–44.

Liu, W., Yi, Z., Xu, D., Clamp, J.C., Li, J., et al., 2015. Two new genera of planktonic ciliates and insights into the evolution of the family Strombidiidae (Protista, Ciliophora, Oligotrichia). PLoS One 10: e0131726.

Luo, Z., Lim, Z.F., Mertens, K.N., Gurdebeke, P.R., Bogus, K., Carbonell-Moore, M.C., Vrielinck, H., Leaw, C.P., Lim, P.T., Chomérat, N., et al. 2018. Morphomolecular diversity and phylogeny of *Bysmatrum* (Dinophyceae) from the South China Sea and France. Eur. J. Phycol. 53, 318–335.

Lynn, D.H., 2008. *The Ciliated Protozoa. Characterization, Classification, and Guide to the Literature*. Springer, Verlag Dordrecht

Mangot, J.F., Domaizon, I., Taib, N., Marouni, N., Duffaud, E., Bronner, G., Debroas, D., 2013. Short-term dynamics of diversity patterns: evidence of continual reassembly within lacustrine small eukaryotes. Environ. Microbiol. 15, 1745–1758.

Marshall, C.P., Javaux, E.J., Knoll, A.W., Walter, M.R., 2005. Combined micro-Fourier transform infrared (FTIR) spectroscopy and micro-Raman spectroscopy of Proterozoic acritarchs: A new approach to palaeobiology. Precambrian Res. 138, 208–224.

Martin, F., 1993. Acritarchs: A review. Biol. Rev. 68: 475–538.

Matsuoka, K., Iishi, K., 2018. Marine and freshwater palynomorphs preserved in surface sediments of Osaka Bay, Japan. Bull. Osaka Mus. Nat. Hist. 72, 1–17.

McCarthy, F.M.G., Pilkington, P.M., Volik, O., Heyde, A., Cocker, S.L., 2021. Non-pollen palynomorphs in freshwater sediments and their palaeolimnological potential and selected applications. Geol. Soc. Spec. Publ. 511, 121–150.

Medlin, L.K., Elwood, H.J., Stickel, S., Sogin, M.L., 1988. The characterization of enzymatically amplified eukaryotic 16S-like rRNA-coding regions. Gene 71, 491–499.

Mendelson, C.V., 1987. Acritarchs. In J. Lipps (Ed.), *Fossil Prokaryotes and Protists* (pp. 62–86). Knoxville: University of Tennessee.

Meunier, A., 1910. Microplankton des Mers de Barents et de Kara. Duc d'Orléans. Campagne arctique de 1907. Imprimerie scientifique Charles Bulens: Bruxelles. 355 p. + atlas (XXXVII plates).

Meunier, A.,1919. Microplancton de la Mer flamande. 4^{me} partie. Les Tintinnides et cetera. Mém. Mus. r. Hist. nat. Belg. 8, 59 p.

Meyvisch, P., Gurdebeke, P.R., Vrielinck, H., Mertens, K.N., Versteegh, G., Louwye, S., 2021. Attenuated Total Reflection (ATR) micro-Fourier Transform Infrared (micro-FT-IR) spectroscopy to enhance repeatability and reproducibility of spectra derived from single specimen organic-walled dinoflagellate cysts. Appl. Spectrosc., https://doi.org/10.1177%2F00037028211041172.

Miettienen, A., Head, M.J., Knudsen, K.L., 2014. Eemian sea-level highstand in the eastern Baltic Sea linked to long-duration White Sea connection. Quat. Sci. Rev. 86, 158–174.

Mironova, E.I., Telesh, I.V., Skarlato, S.O., 2014. Ciliates in plankton of the Baltic Sea. Protistology 8, 81–124.

Montenari, M., Leppig, U., 2003. Die Acritarcha: ihre Klassifikation, Morphologie, Ultrastruktur und paläoökologische/paläoögeographische Verbreitung. Palaeontol. Z. 77, 173–194.

Moreira, D., von der Heyden, S., Bass, D., López-García, P., Chao, E., Cavalier-Smith, T., 2007. Global eukaryote phylogeny: Combined small- and large-subunit ribosomal DNA trees support monophyly of Rhizaria, Retaria and Excavata. Mol. Phylogenet. Evol. 44, 255–266.

Moscatello, S., Belmonte, G., 2004. Active and resting stages of zooplankton and its seasonal evolution in a hypersaline temporary pond of the Mediterranean coast (the "Vecchie Salina", SE Italy). Sci. Mar. 68, 491–500.

Mudie, P.J., Marret, F., Rochon, A., Aksu, A.E., 2010. Non-pollen palynomorphs in the Black Sea corridor. Veg. Hist. Archaeobot. 19, 531–544.

Mudie, P., Marret, F., Gurdebeke, P.R., Hartman, J.D., Reid, P.C., 2021. Marine dinocysts, acritarchs and less well-known NPP: tintinnids, ostracod and foraminiferal linings, copepod and worm remains. Geol. Soc. Spec. Publ. 511, 159–232.

Nehring, S., 1994. Spatial distribution of dinoflagellate resting cysts in recent sediments of Kiel Bight, Germany (Baltic Sea). Ophelia 39, 137–158.

Ning, W., Andersson, P.A., Ghosh, A., Khan, M., Filipsson, H.L., 2017. Quantitative salinity reconstructions of the Baltic Sea during the mid-Holocene. Boreas 46, 100–110.

Penard, E., 1922. *Etudes sur les infusoires d'eau douce*. Geneve, Georg & Cie, 331 p.

Pienkowski, A.J., Kennaway, S., Lang, S.I., 2020. Aquatic palynomorphs from modern marine sediments in a reconnaissance transect across the Northwest Passage – Baffin Bay region. Mar. Micropaleontol. 156, 101825.

Pospelova, V., Pedersen, T.F., de Vernal, A., 2006. Dinoflagellate cysts as indicators of climatic and oceanographic changes during the past 40 kyr in the Santa Barbara Basin, southern California. Paleoceanography 21, 1–16.

Pospelova, V., Esenkulova, S., Johannessen, S.C., O'Brien, M.C., Macdonald, R.W., 2010. Organic-walled dinoflagellate cyst production, composition and flux from 1996 to 1998 in the central Strait of Georgia (BC, Canada): A sediment trap study. Mar. Micropaleontol. 75, 17–37.

Price, A.M., Pospelova, V., 2011. High-resolution sediment trap study of organic-walled dinoflagellate cyst production and biogenic silica flux in Saanich Inlet (BC, Canada). Mar. Micropaleontol. 80, 18–43.

Price, A.M., Gurdebeke, P.R., Mertens, K.N., Pospelova, V., 2016. Determining the absolute abundance of dinoflagellate cysts in recent marine sediments III: identifying the source of *Lycopodium* loss during palynological processing and further testing of the *Lycopodium* marker-grain method. Rev. Palaeobot. Palynol. 226, 78–90.

Rambaut, A., 2009. FigTree v. 1.2.3. Available at http://tree.bio.ed.ac.uk/software/figtree/

Reid, P.C., 1972. The distribution of dinoflagellate cysts, acritarchs and pollen in coastal sediments from the British Isles. Unpublished PhD thesis, University of Sheffield.

Reid, P.C., John, A.W.G., 1978. Tintinnid cysts. J. Mar. Biolog. Assoc. U.K. 58, 551–557.

Reid, P.C., John, A.W.G., 1983. Resting cysts in the ciliate class Polyhymenophorea: Phylogenetic implications. J. Protozool. 30, 710-713.

Ronquist, F., Teslenko, M., van der Mark, P., Ayres, D.L., Darling, A., Höhna, S., Larget, B., Liu, L., Suchard, M.A., Huelsenbeck, J.P., 2012 MrBayes 3.2: efficient Bayesian phylogenetic inference and model choice across a large model space. Syst. Biol. 61, 539–542.

Rubino, F., Moscatello, S., Belmonte, M., Ingrosso, G., Belmonte, G., 2013. Plankton resting stages in the marine sediments of the Bay of Vlorë (Albania). Int. J. Ecol., 101682.

Rubino, F., Belmonte, G., 2019. A new cyst morphotype from Recent sediments of the Mar Piccolo of Taranto (Southern Italy, Ionian Sea). Prog. Aqua Farming Mar. Biol. 2, 180015.

Santoferrara, L.F., Alder, V.V., McManus, G.B., 2017. Phylogeny, classification and diversity of Choreotrichia and Oligotrichia (Ciliophora, Spirotrichea). Mol Phylogenet Evol. 112: 12-22.

Sela, I., Ashkenazy, H., Katoh, K., Pupko, T., 2015. GUIDANCE2: accurate detection of unreliable alignment regions accounting for the uncertainty of multiple parameters. Nucleic Acids Res. 43: W7–W14.

Shatilovich, A., Stoupin, D., Rivkina, E., 2015. Ciliates from ancient permafrost: Assessment of cold resistance of the resting cysts. Eur. J. Protistol. 51, 230–240.

Shimano, S., Sambe, M., Kasahara, Y., 2012. Application of nested PCR-DGGE (denaturing gradient gel electrophoresis) for the analysis of ciliate communities in soils. Microbes Environ. 27, 136–141.

Song, W., Pan, B., El-Serehy, H.A., Al-Farraj, S.A., Liu, W., Li, L., 2020. Morphology and Molecular phylogeny of two freshwater oligotrich ciliates (Protozoa, Ciliophora, Oligotrichia), *Pelagostrombidium fallax* (Zacharias, 1895) Krainer, 1991 and *Limnostrombidium viride* (Stein, 1867) Krainer, 1995, with brief notes on stomatogenesis. J. Eukaryot. Microbiol. 67, 232–244.

Sonnenberg, R., Nolte, A.W., Tautz, D., 2007. An evaluation of LSU rDNA D1-D2 sequences for their use in species identification. Front. Zool. 4, 6.

Sorrel, P., Popescu, S.M., Head, M.J., Suc, J.P., Klotz, S., Oberhänsli, H., 2006. Hydrographic development of the Aral Sea during the last 2000 years based on a quantitative analysis of dinoflagellate cysts. Palaeogeogr. Palaeoclimatol. Palaeoecol. 234, 304–327.

Telesh, I., Postel, L., Heerklozz, R., Mironova, E., Skarlato, S., 2009. Zooplankton of the open Baltic Sea: Extended atlas. Meereswiss. Ber. 76, 290 p.

Van Hauwaert, T., 2016. Recent dinoflagellate cysts from the Chesapeake estuary (Maryland and Virginia, U.S.A.): taxonomy and ecological preferences. Unpublished master's dissertation, Ghent University, 91 p.

Van Waveren, I.M., Marcus, N.H., 1993. Morphology of recent copepod egg envelopes from Turkey Point, Gulf of Mexico, and their implications for acritarch affinity. Spec. Pap. Palaeontol. 48, 111–24.

Vďačný, P., Foissner, W., 2012. Monograph of the Dileptids (Protista, Ciliophora, Rhynchostomatia). *Denisia* 31, 1–529.

Verhoeven, K., Louwye, S., Paez-Reyes, M., Mertens, K.N., Vercauteren, D., 2014. New acritarchs from the late Cenozoic of the southern North Sea Basin and the North Atlantic realm. Palynology 38, 38–50.

Vermeiren, M., 1983. Resten met organische wand van recente micro-organismen in waddenafzettingen aan de zuidoostrand van Schiermonnikoog. Thesis licentiate zoology, Ghent University, 100 p.

Verni, F., Rosati, G., 2011. Resting cysts: A survival strategy in Protozoa Ciliophora. Ital. J. Zool. 78, 134-145.

Viherluoto, M., Kuosa, H., Flinkman, J., Viitasalo, M.,. 2000. Food utilisation of pelagic mysids, *Mysis mixta* and *M. relicta*, during their growing season in the northern Baltic Sea. Mar. Biol. 136, 553–559.

Wailes, G.H., 1928. Fresh water and marine Protozoa from British Columbia, with descriptions of new species. Vancouver Museum and Art Notes 3, 25–31.

Wall, D., 1962. Evidence from Recent Plankton Regarding the Biological Affinities of *Tasmanites* Newton 1875 and *Leiosphaeridia* Eisenack 1958. Geol. Mag. 99, 353–362.

Wang, Z., Matsuoka, K., Qi, Y., Chen, J., Lu, S., 2004. Dinoflagellate cyst records in recent sediments from Daya Bay, South China Sea. Phycological Res. 52, 396–407.

Wright, R.R., 1907. The plankton of eastern Nova Scotia waters. An account of floating organisms upon which young food-fishes mainly subsist. Contrib. Can. Biol. Fish. 1, 1–19.

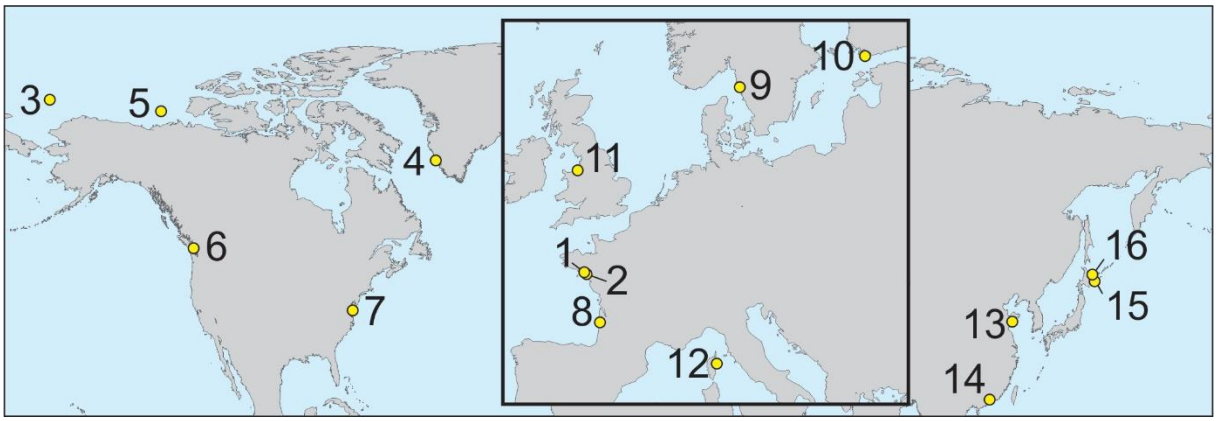

Fig. 1. Sample locations of the material studied in this paper. 1. Vilaine Bay (France), 2. Pornichet (France), 3. Chukchi Sea, 4. Labrador Sea, 5. Beaufort Sea, 6. Saanich Inlet (B.C., Canada), 7. Chesapeake Bay (USA), 8. Gironde (France), 9. Galterö (Sweden), 10. Båthusfjärden (Finland), 11. Dee Estuary (UK), 12. Diana Lagoon (Corsica), 13. Qingdao (China), 14. Daya Bay (China), 15. Akkeshi Bay (Japan), 16. Lake Saroma (Japan). See Table 2 for details.

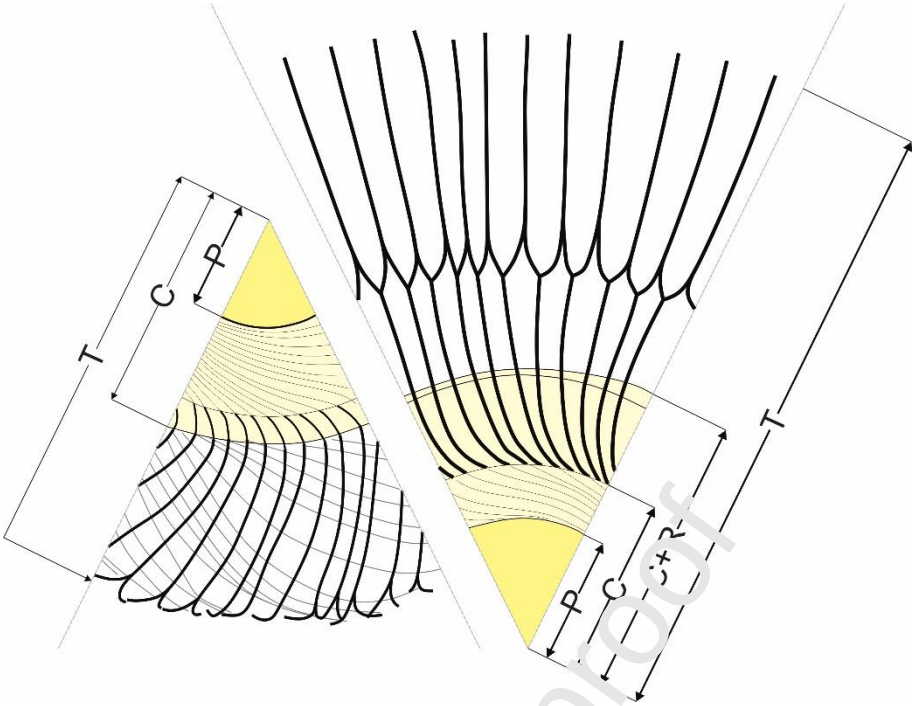

Fig. 2. Schematic drawing of (sectors of) *Radiosperma textum* (left) and *R. corbiferum* (right). P = excystment pore (pylome) diameter; C = central body diameter; C+R = central body + ring-shaped region; T = total diameter.

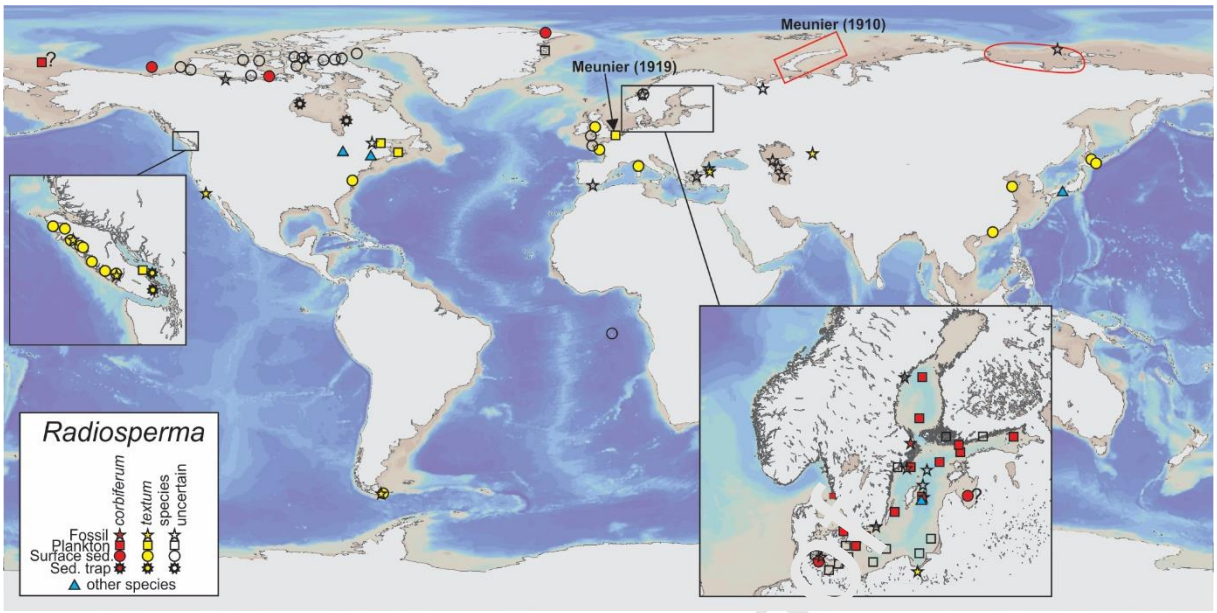

Fig. 3. Global distribution of all known *Radiosperma* species, as fossil, in modern sediments, in sediment traps and in plankton (symbol shape). Color-filled symbols represent records in literature which are substantiated with illustrations, supplemented with personal observations. Unfilled symbols were not confirmed (i.e. *Radiosperma* sp.). Blue triangles represent reports of other, undescribed species which probably belong to *Radiosperma*. A source with closely spaced observation points is represented by a single point. A question mark indicates an uncertain geographical position. The substantiated records are included in the synonymy lists in section 3.1.

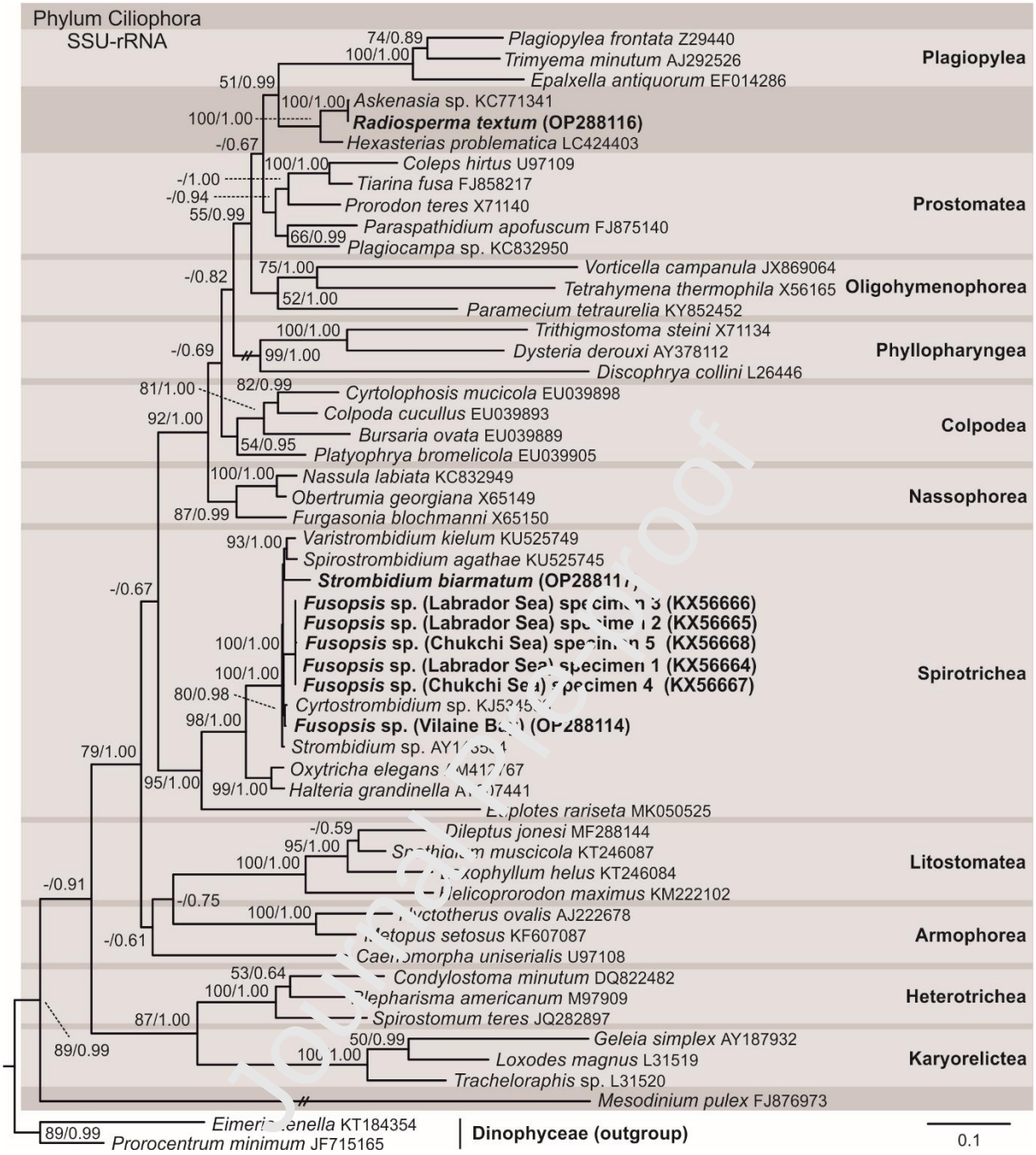

Fig. 4. Phylogenetic SSU-rRNA placement of *Strombidium biarmatum*, *Fusopsis* sp. (Labrador Sea, Chukchi Sea and Vilaine Bay) and *Radiosperma textum* within phylum Ciliophora. According to the existing classification (e.g., Adl et al. 2019). Bootstrap values for the maximum likelihood (ML) and posterior probabilities for the Bayesian inference (BI) were mapped onto the best ML tree. A dash indicates node support values below 50%. Sequences in boldface were obtained during this study. The scale bar indicates one substitution per ten nucleotide positions.

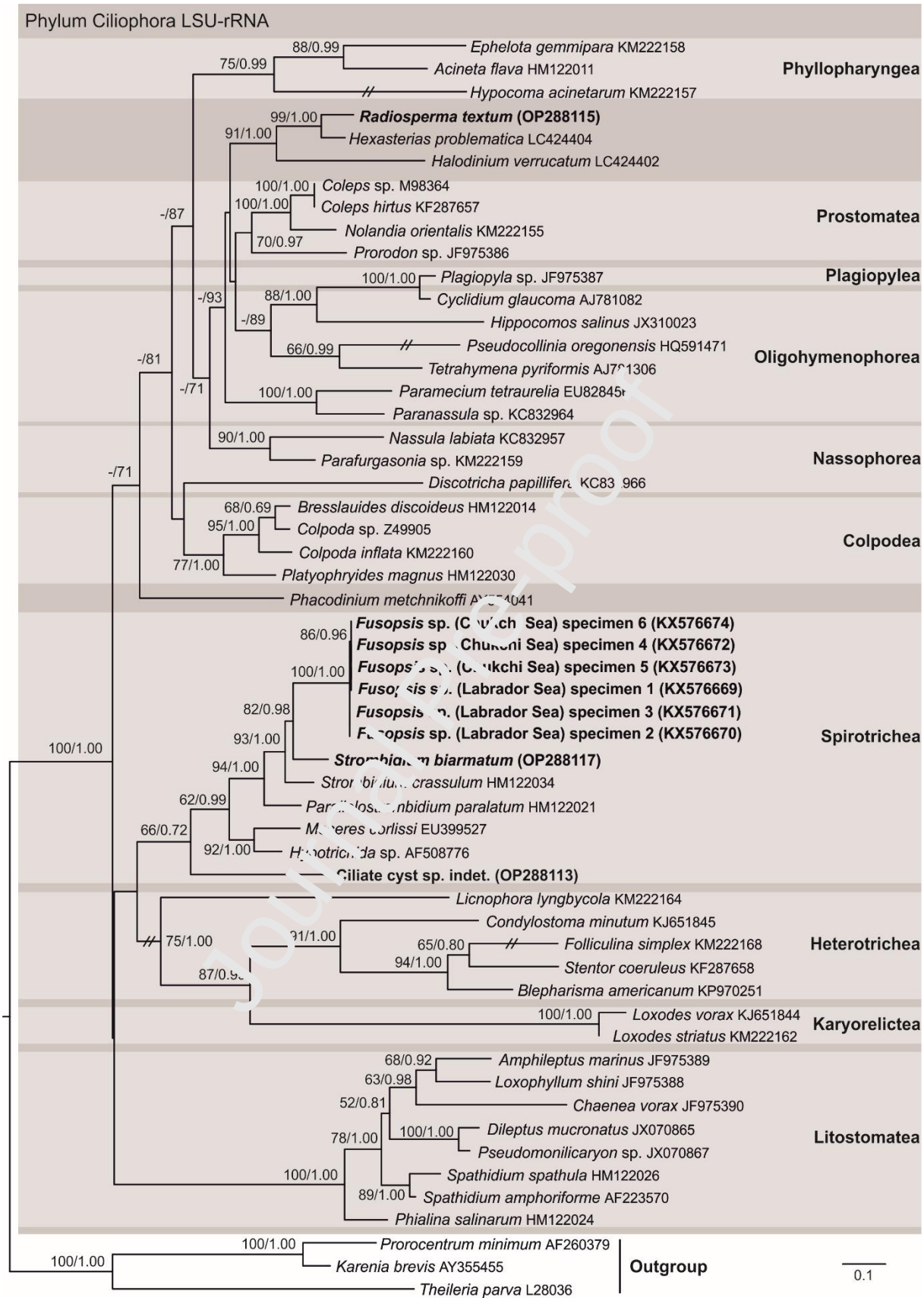

Fig. 5. Phylogenetic LSU-rRNA placement of *Strombidium biarmatum*, Ciliate cyst sp. indet, sp., *Fusopsis* sp. (Labrador Sea and Chukchi Sea) specimens 1–6, and *Radiosperma textum*

within phylum Ciliophora. According to the existing classification (e.g., Adl et al. 2019). Bootstrap values for the maximum likelihood (ML) and posterior probabilities for the Bayesian inference (BI) were mapped onto the best ML tree. A dash indicates node support values below 50%. Sequences in boldface were obtained during this study. The scale bar indicates one substitution per ten nucleotide positions.

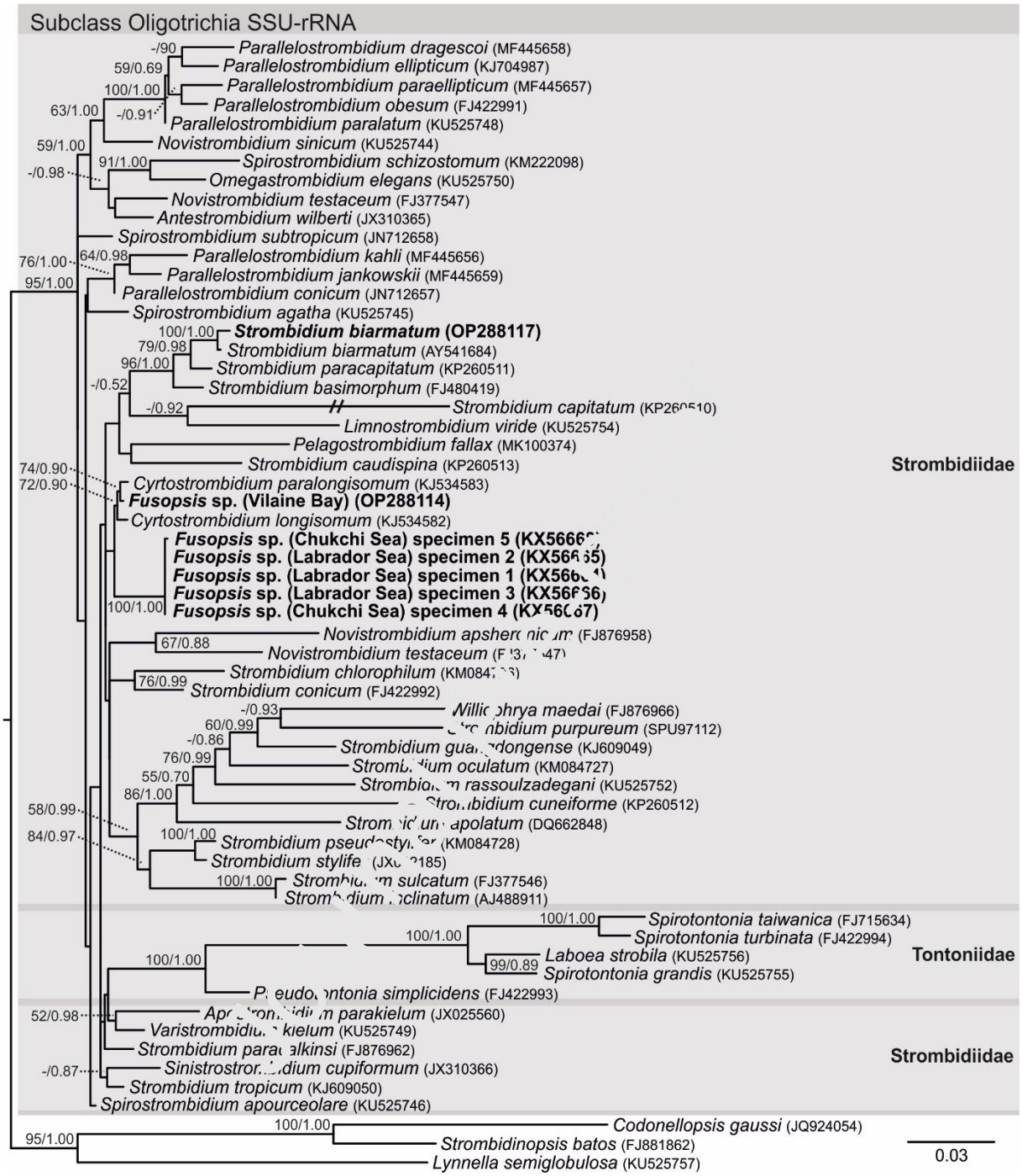

Fig. 6. Phylogenetic SSU-rRNA placement of *Strombidium biarmatum* and *Fusopsis* sp. (Vilaine Bay, Chukchi Sea and Labrador Sea) within the subclass Oligotrichia. According to the alignment and classification in Song et al. (2020). Bootstrap values for the maximum likelihood (ML) and posterior probabilities for the Bayesian inference (BI) were mapped onto the best ML tree. A dash indicates node support values below 50%. Sequences in boldface were obtained during this study. The scale bar indicates three substitutions per one hundred nucleotide positions.

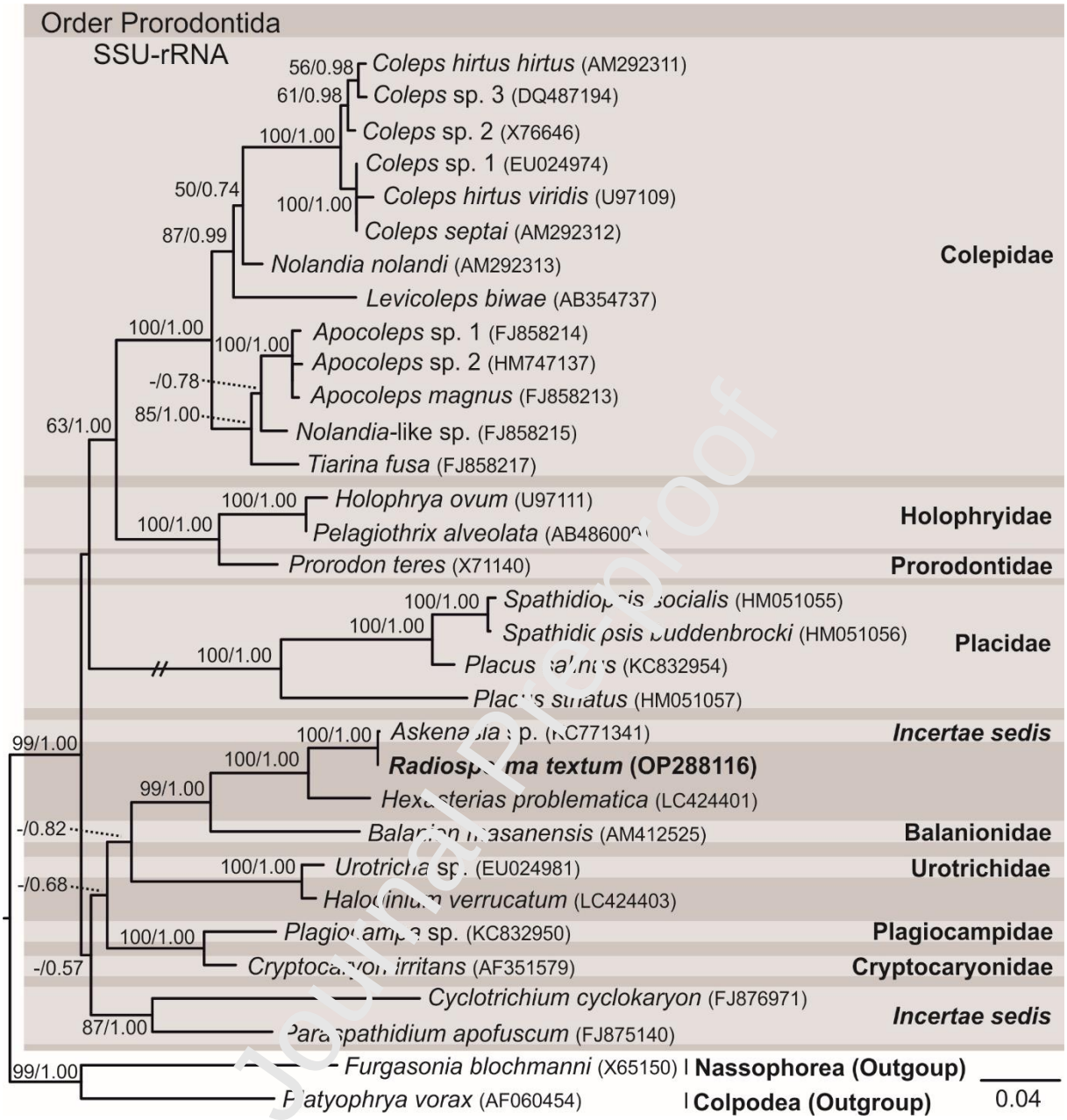

Fig. 7. Phylogenetic SSU-rRNA placement of *Radiosperma textum* within the order Prorodontida. According to the alignment and classification in Gurdebeke et al. (2018a). Bootstrap values for the maximum likelihood (ML) and posterior probabilities for the Bayesian inference (BI) were mapped onto the best ML tree. A dash indicates node support values below 50%. Sequences in boldface were obtained during this study. The scale bar indicates four substitutions per one hundred nucleotide positions.

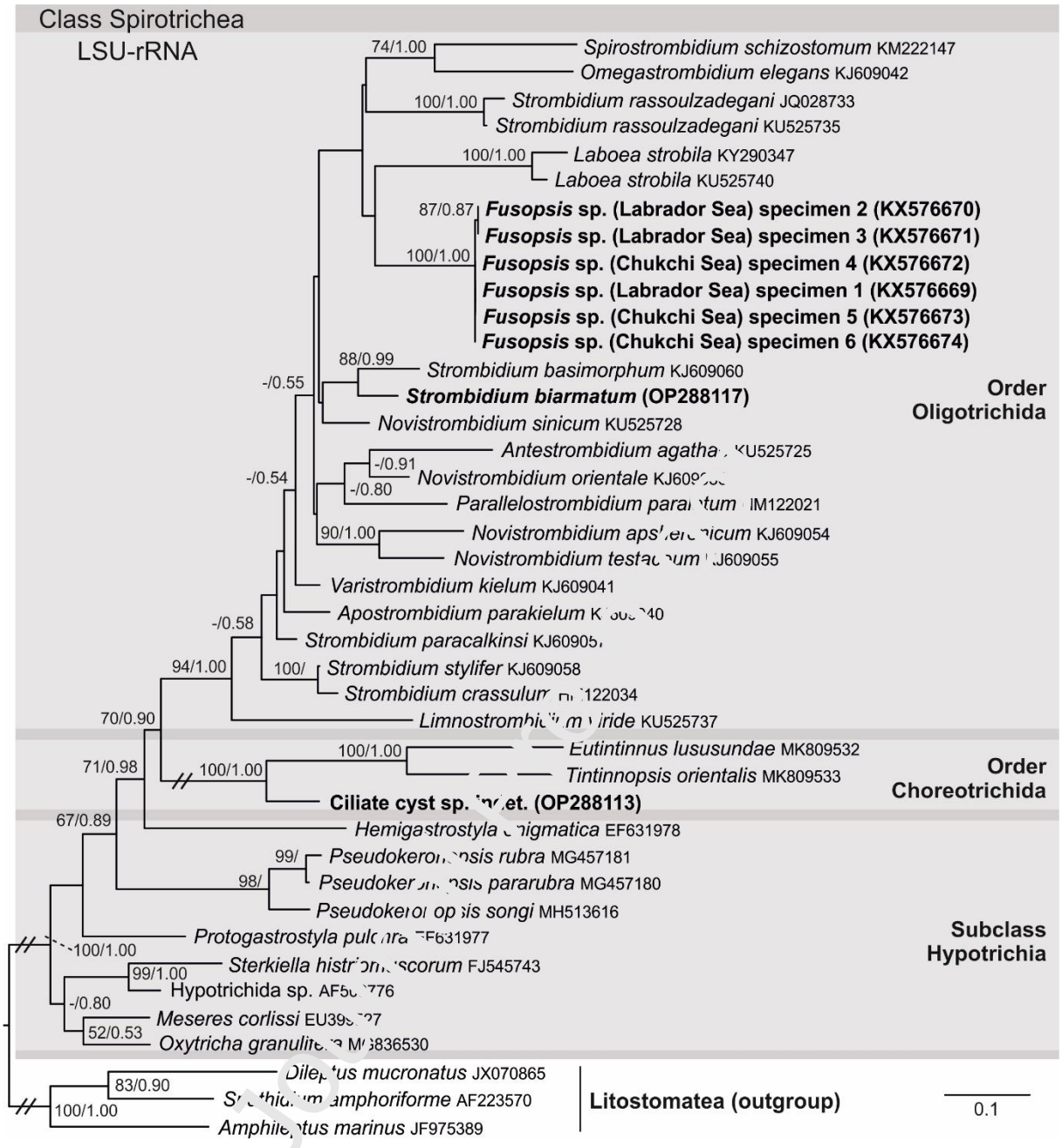

Fig. 8. Phylogenetic LSU-rRNA placement of *Strombidium biarmatum*, *Fusopsis* sp. (Labrador Sea and Chukchi Sea), and Ciliate cyst sp. indet. within the class Spirotrichea. According to the existing classification (e.g., Adl et al. 2019). Bootstrap values for the maximum likelihood (ML) and posterior probabilities for the Bayesian inference (BI) were mapped onto the best ML tree. A dash indicates node support values below 50%. Sequences in the boldface were obtained during this study. The scale bar indicates one substitution per ten nucleotide positions.

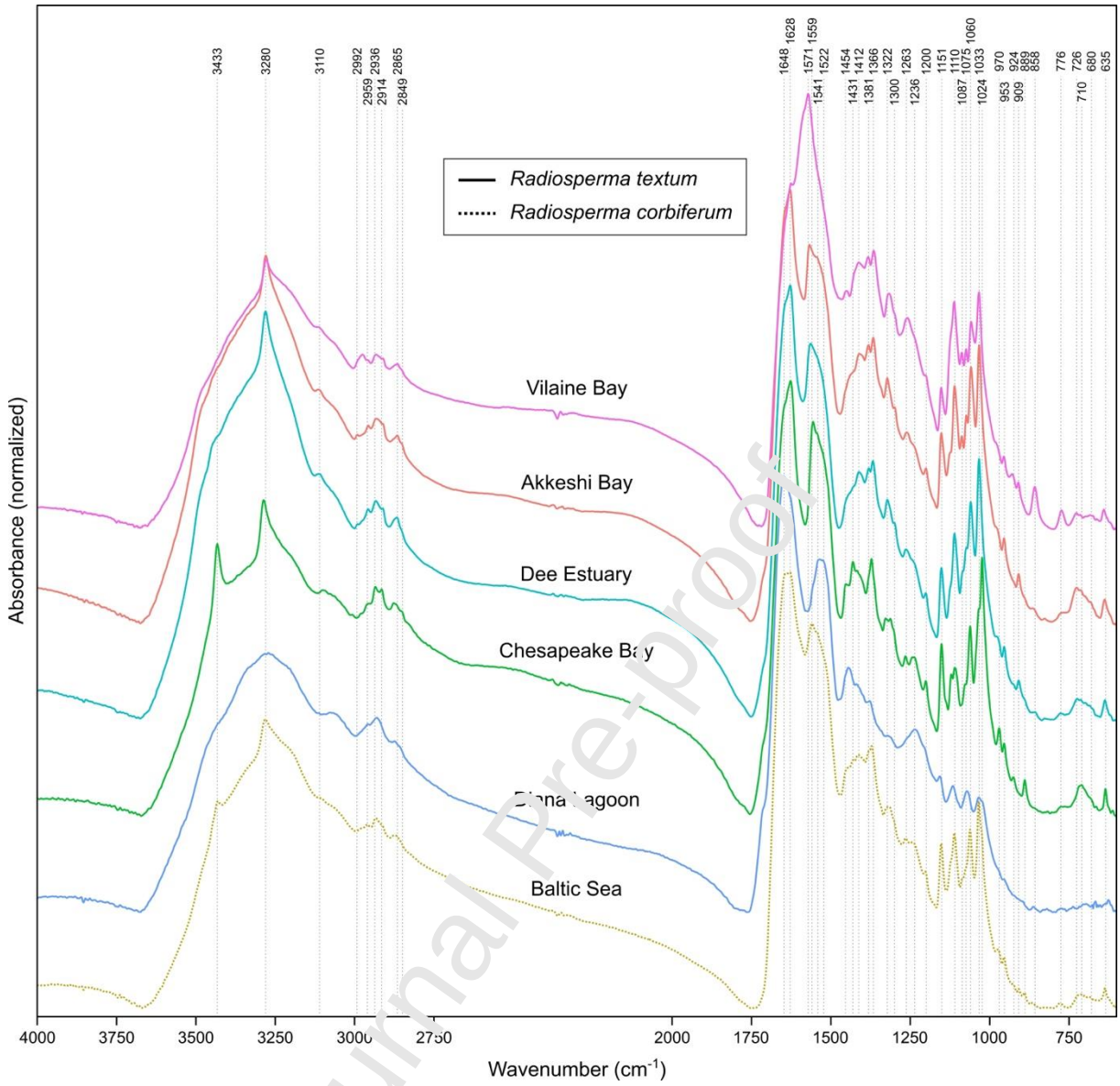

Fig. 9. Averaged and normalized micro-FTIR spectra of *Radiosperma textum* (solid lines) and *R. corbiferum* (dotted line) from several estuarine settings in the Northern Hemisphere: Vilaine Bay (2), Akkeshi Bay (11), Dee Estuary (4) and Chesapeake Bay (6), Diana lagoon (1) and the Baltic Sea. Spectra from Gurdebeke et al. (2018a) are included.

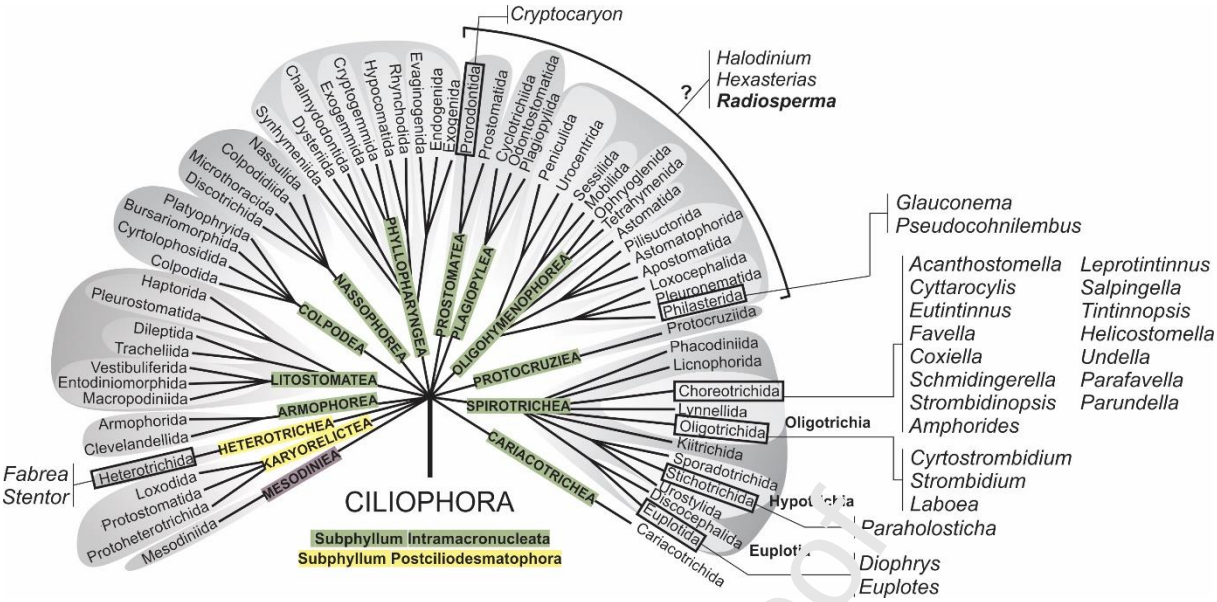

Fig. 10. Phylogeny of the Ciliophora as presented by Gao et al. (2016) and modified after Adl et al. (2019), with the position of marine taxa that produce resting cysts.

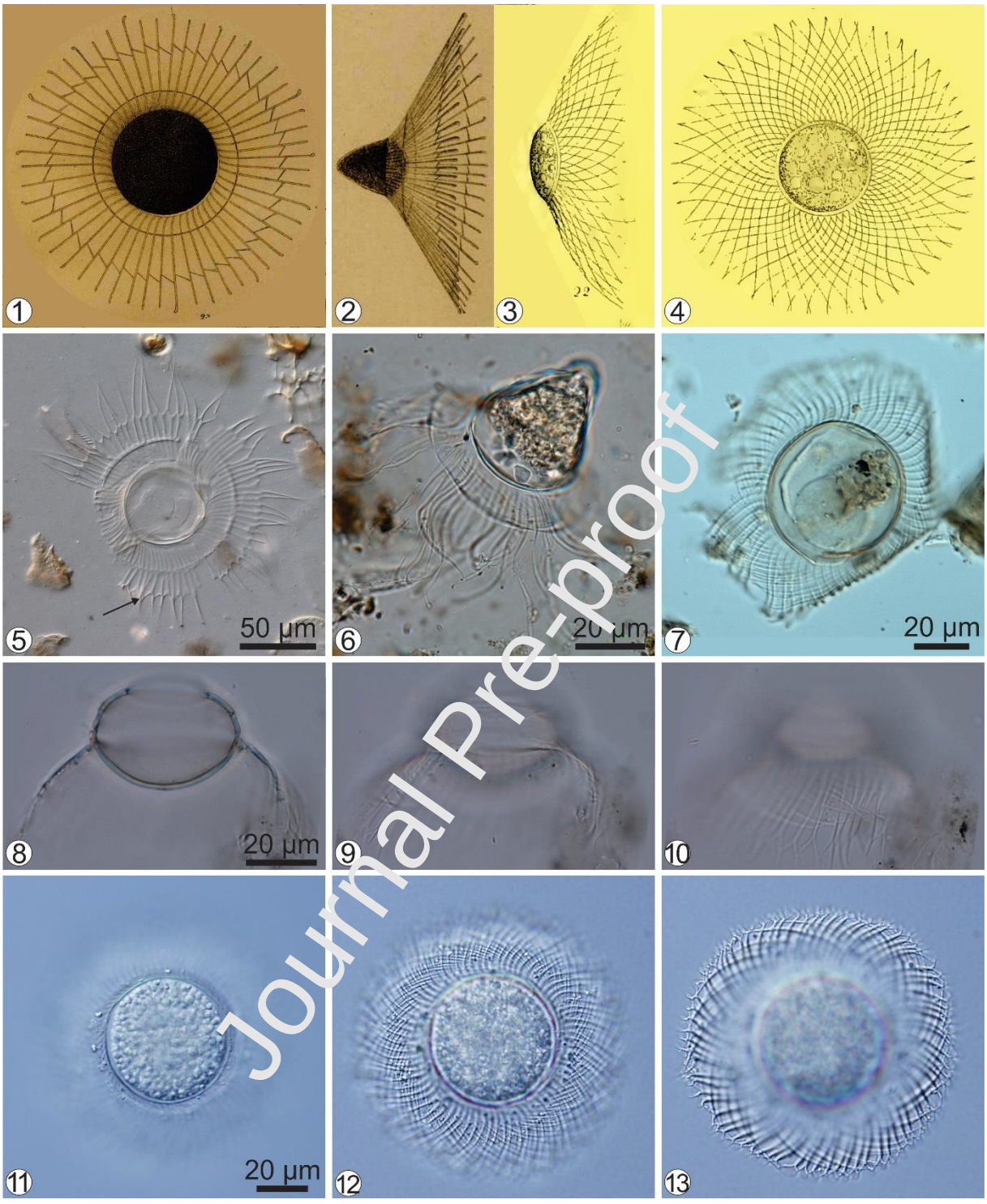

Plate 1. Illustrations and LM images of *Radiosperma corbiferum* (1-2, 5-6) and *R. textum* (3-4, 7-13). 1-2. *R. corbiferum*, line drawings from Hensen (1887) (as "Sternhaarstatoblast"); 3-4. *R. textum*, line drawings from the original description in Meunier (1919). 5. Båthusfjärden, Finland; arrow points at vacuoles. 6. Beaufort Sea. 7. Neroutsos Inlet, Vancouver Island

(surface sediment, sample 12-136 in Gurdebeke et al. 2018c). 8–10. Daya Bay (South China Sea). 11–13. Lake Saroma (photo by Yoshihito Takano).

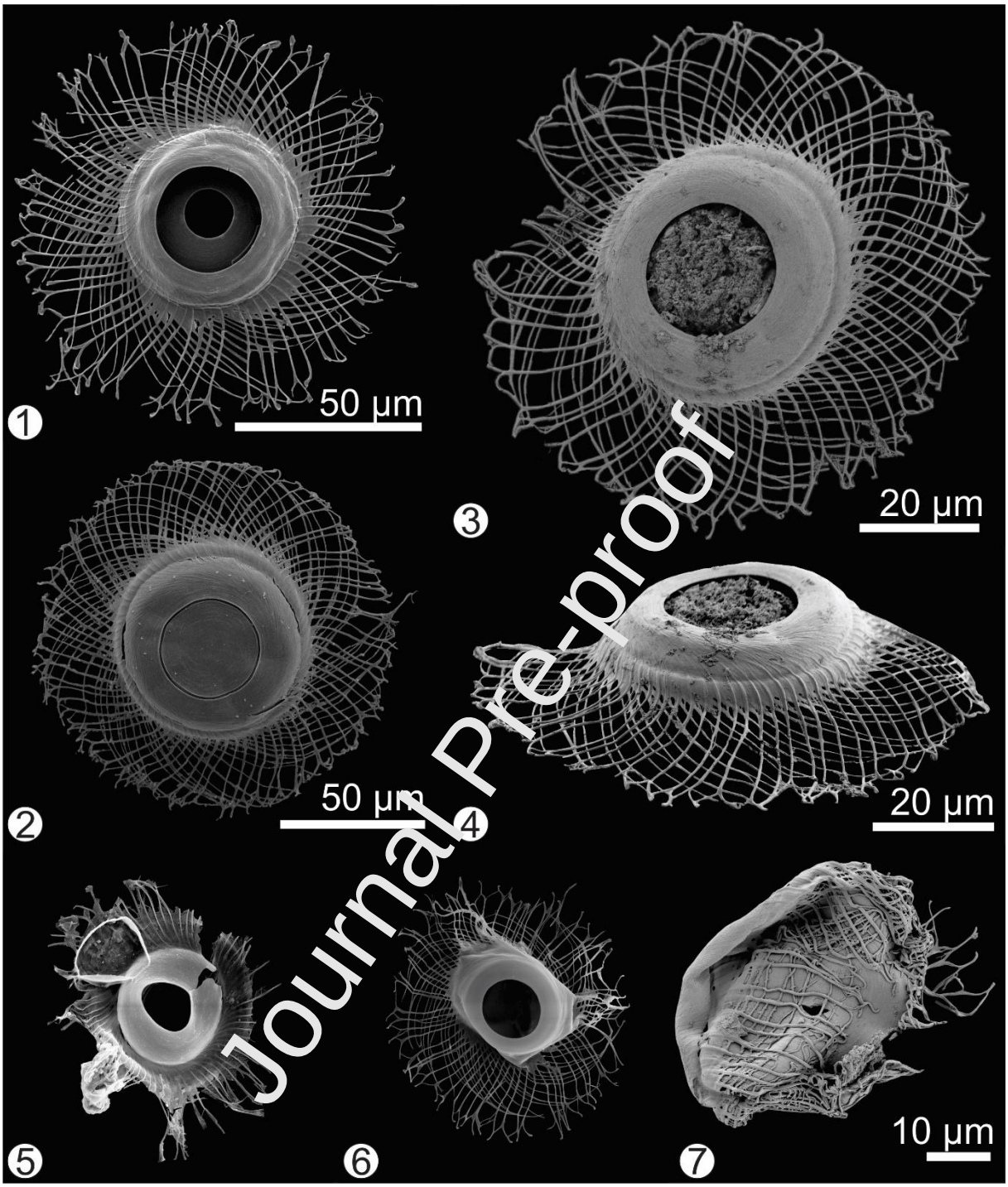

Plate 2. SEM micrographs of *Radiosperma textum* (1–4, 6, 7) and *R. corbiferum* (5). 1. Vilaine Bay, Brittany, France. Polar view, showing secondary opening through archeopyle; 2. Gironde, France. Polar view, showing closed pylome with preformed operculum. 3–4. Saanich Inlet, B.C., Canada. 3. Polar view. 4. Oblique polar view. 5-6. Galterö, Sweden. Polar view of both *R. corbiferum* (5) and *R. textum* (6) occurring in one sample. 7. Saanich Inlet. Crushed specimen.

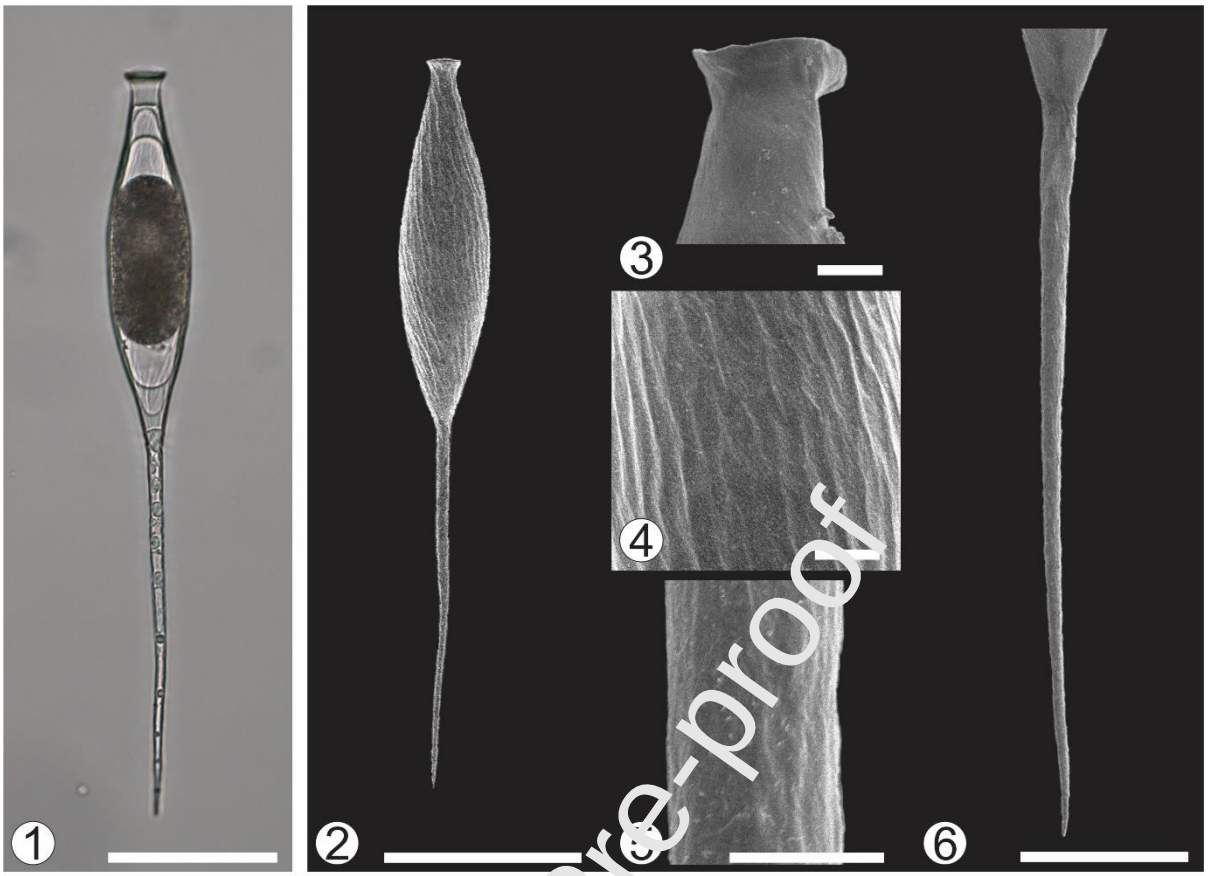

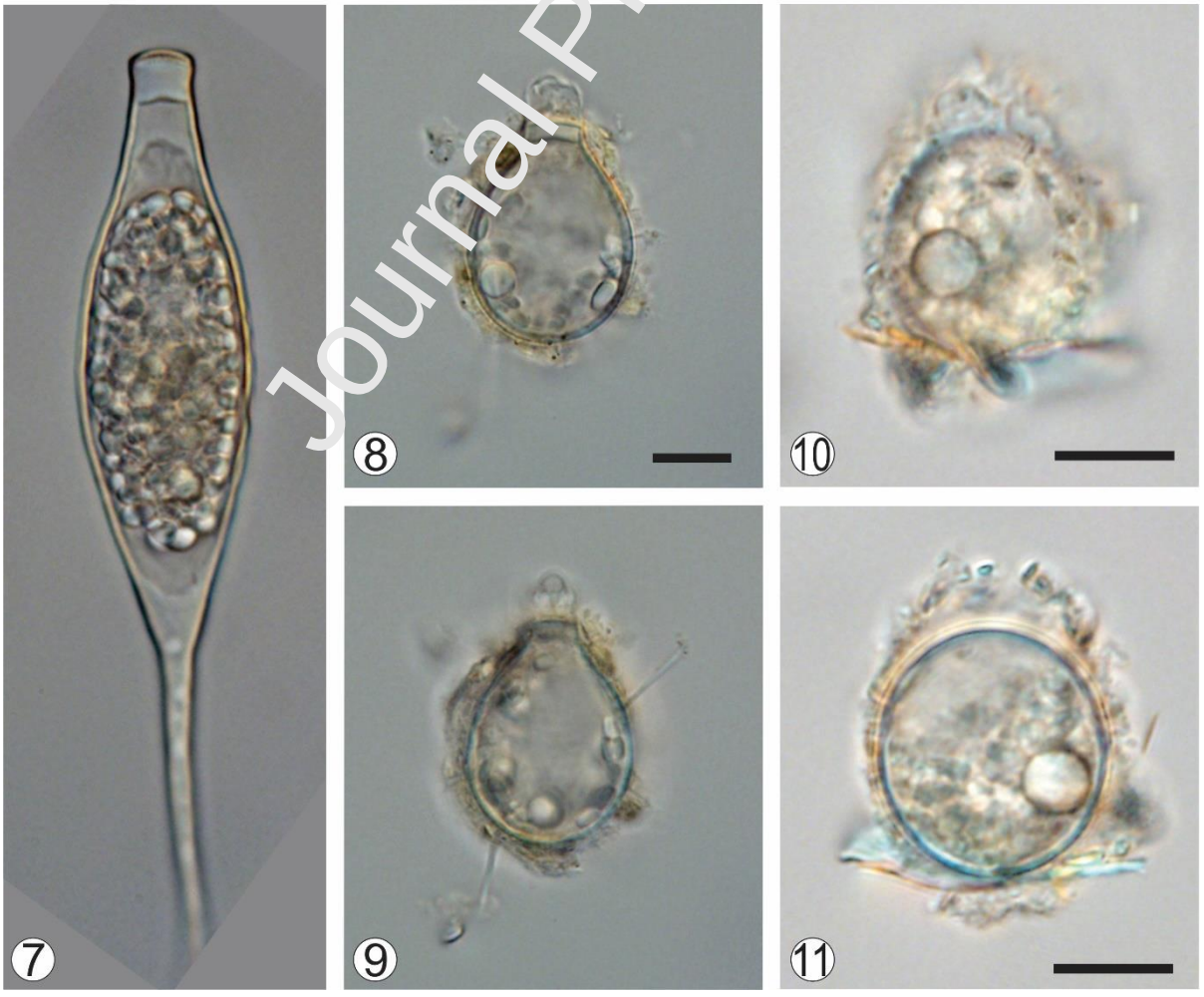

Plate 3. Spirotrich ciliate cysts. 1–7: *Fusopsis* sp. specimens collected in surface sediment samples from the Chukchi Sea (1, 3, 4, 6), Labrador Sea (2, 4) and Vilaine Bay (7). 1. Light micrograph of living cyst with granular cell content and a long spine containing droplets; 2. SEM micrograph of general view of the cyst depicting the oblique and parallel striations at the surface; 3. SEM micrograph of details of the papula located at the apical extremity of the cyst; 4. SEM micrograph of details of the striation at the surface of the cyst; 5. SEM micrograph of surface of the spine. 7. LM of living cyst containing lipid bodies. 8–9: *Strombidium* cf. *biarmatum*. 10–11: Ciliate cyst sp. indet. Scale bars = 100 μm (1, 2), 50 μm (6), 10 μm (3, 4, 8–11), and 5 μm (5).

Table 1. Sample locations the material used in this study, with indication of sampling date, coordinates, water depth and, where relevant, references in which the samples were studied previously.

Location	Taxa identified	Date	Longitude	Latitude	Water depth	Reference
Vilaine Bay, France	*Radiosperma textum*, *Strombidium biarmatum*, *Fusopsis* sp.	January 15, 2019	47.4620°N	2.5006° W	5.6 m	Gurdebeke et al. (2018a)
Pornichet, France	Ciliate cyst sp. indet.	January 22, 2019	47.2579°N	2.3508° W	5.0 m	This study
Chukchi Sea	*Fusopsis* sp.	September 6, 2015	73.6317°N	166.5198° W	104 m	This study
Labrador Sea	*Fusopsis* sp.	August 3, 2015	63.5540°N	52.2187 °W	506 m	This study
Beaufort Sea	*Radiosperma corbiferum*	January 2015	71.0021°N	135.5094°W	700 m	This study
Saanich Inlet, BC, Canada	*Radiosperma textum*	Summer 2012	48.5926°N	123.5006°W	226 m	Price et al. (2016)
York River, Chesapeake Bay, USA	*R. textum*	July 10, 2014	37.2927°N	76.5347 °W	n.a.	Van Hauwaert (2016)
Gironde, France	*R. textum*	April 15 and 19, 2016	44.6364°N	1.0667° W	1.5 m	Luo et al. (2018)
Galterö, Sweden	*R. textum*, *R. corbiferum*	May 2010	57.11° N	11.81°E	40.5 m	Gurdebeke et al. (2018a)
Båthusfjärden, Finland	*R. corbiferum*	2007	59.92° N	22.98°E	9.2 m	This study
Mooreside saltmarsh (off Neston, Dee Estuary), UK	*R. textum*	February 6, 2014	53.2881°N	3.1044° E	1.0 m	Gurdebeke et al. (2018b)
Diane Lagoon, Corsica	*R. textum*	January 18, 2016	42.1277°N	9.5287° E	9.0 m	Gu et al. (2021)
Qingdao, China	*R. textum*	May 8, 2011	36.0830°N	120.3019°E	9.8 m	This study
Daya Bay, China	*R. textum*	August 2001	114.5303°N	22.5692 °E	5.0 m	Wang et al. (2004)
Akkeshi Bay, Japan	*R. textum*	July 21, 2011	43.0669°N	144.8638°E	1.0 m	Jansegers (2019)
Lake Saroma, Japan	*R. textum*	July 22, 2011	44.1226°N	143.8742°E	18.3 m	This study

Table 2. Morphometrics of Radiosperma corbiferum and Radiosperma textum. Data for R. corbiferum includes measurements compiled from literature (see text).

Trait	Average	N	Min.	Max.	σ	Average	N	Min.	Max.	σ
Total diameter (µm)	159.6	6	90.0	200.0	28.7	102.6	5	95.3	108.0	4.8
Central body diameter (µm)	47.5	4	42.0	55.5	5.0	44.7	11	33.2	54.5	5.4
Central body + annulus diameter (µm)	78.7	4	70.6	84.9	5.1	-	-	-	-	-
Flange width (µm)	43.6	2	29.5	57.6	14	26.3	7	21.6	33.7	4.2
Pylome diameter (µm)	38.0	-	25.0	40.0	-	25.2	10	21.7	28.3	2.2
Secondary pylome diameter (µm)	-	-	-	-	-	10.2	3	8.7	13.1	2.1

Author statement for MARMIC-D-22-00051

Authors: Pieter R. Gurdebeke (PRG), Kenneth Neil Mertens (KNM), Lubomir Rajter (LR), Pjotr Meyvisch (PM), Eric Potvin (EP), Eun Jin Yang (EJY), Coralie André (CA), Vera Pospelova (VP), Stephen Louwye (SL)

Conceptualization: PG, KM;

Data curation: PG, KM, LR, PM;

Formal analysis: PG, KM, LR, PM;

Funding acquisition: KNM, EJY;

Investigation: PG, KM, LR, PM, EP, EJY, CA, VP;

Methodology: PG, KM, EP, EJY;

Project administration: PG, KM, SL;

Resources: PG, KM, EP, VP;

Software: PG, LR, PM;

Supervision: KM, SL;

Validation: PRG, KNM, PM, EP;

Visualization: PG, KM, PM, EP;

Writing - original draft: PG, KM, LR, PM, EP, EJY, VP, SL.

Writing - review & editing: PG, KM, LR.

Declaration of interests

The authors declare that there are no conflicts of interest.

☐The authors declare that they have no known competing financial interests or personal relationships that could have appeared to influence the work reported in this paper.

☒The authors declare the following financial interests/personal relationships which may be considered as potential competing interests:

Eun Jin Yang reports financial support was provided by Ministry of Oceans and Fisheries, Korea. Kenneth Neil Mertens reports financial support was provided by French National Research Agency (ANR) and the Agence de l'Eau Loire-Bretagne

Highlights:

- Former acritarch *Radiosperma* and its two species *R. corbiferum* and *R. textum* are redescribed as ciliates.
- *Radiosperma corbiferum* is confined to Baltic and Arctic waters while *R. textum* occurs elsewhere.
- *Radiosperma textum* is a ciliate cyst based on rRNA.
- Ciliate cyst morphology has taxonomic significance.